nature cell biology

Bmi1 is essential in Twist1-induced epithelial–mesenchymal transition

Muh-Hwa Yang[1,2,3,4,11,12], Dennis Shin-Shian Hsu[1,11], Hsei-Wei Wang[1,4,5], Hsiao-Jung Wang[1], Hsin-Yi Lan[1], Wen-Hao Yang[1], Chi-Hung Huang[6], Shou-Yen Kao[7], Cheng-Hwai Tzeng[3], Shyh-Kuan Tai[8], Shyue-Yih Chang[4,8], Oscar Kuang-Sheng Lee[1,9] and Kou-Juey Wu[4,10,12]

The epithelial–mesenchymal transition (EMT), one of the main mechanisms underlying development of cancer metastasis, induces stem-like properties in epithelial cells. Bmi1 is a polycomb-group protein that maintains self-renewal, and is frequently overexpressed in human cancers. Here, we show the direct regulation of *BMI1* by the EMT regulator, Twist1. Furthermore, Twist1 and Bmi1 were mutually essential to promote EMT and tumour-initiating capability. Twist1 and Bmi1 act cooperatively to repress expression of both E-cadherin and p16INK4a. In patients with head and neck cancers, increased levels of both Twist1 and Bmi1 correlated with downregulation of E-cadherin and p16INK4a, and was associated with the worst prognosis. These results suggest that Twist1-induced EMT and tumour-initiating capability in cancer cells occurs through chromatin remodelling, which leads to unfavourable clinical outcomes.

The epithelial–mesenchymal transition (EMT) is a developmental process in which epithelial cells lose their polarity and acquire the migratory properties of mesenchymal cells. EMT has been shown to be the pivotal mechanism contributing to cancer metastasis[1]. A recent breakthrough in metastasis research revealed that induction of EMT also generates cells with stem-like properties[2,3]. This finding provides a crucial link between the acquisition of metastatic traits and tumour-initiating capability in cancer cells undergoing EMT. Although the phenotypic association between EMT and tumour-initiating properties is firmly established, the underlying molecular mechanisms remain largely unknown.

Bmi1 is a member of the polycomb-repressive complex 1 (PRC1) that has an essential role in maintaining chromatin silencing[4,5]. Bmi1 is involved in the self-renewal of neuronal, haematopoietic and intestinal cells through repression of the *INK4A–ARF* locus[6–10]. Repression of *INK4A–ARF* by Bmi1 is polycomb-repressive complex 2 (PRC2)-dependent. Binding of PRC2 to its target genes allows EZH2, a subunit of PRC2, to methylate Lys 27 of histone H3 (H3K27)[11,12]. PRC1 recognizes trimethylated H3K27 (H3K27me3) and maintains the repression of target genes[13,14]. In human cancers, Bmi1 and c-Myc function together to promote lymphomagenesis[15], and overexpression of *BMI1* is frequently observed in tumour-initiating cells[16–18]. However, the regulatory mechanism of Bmi1 in cancer cells and its role in metastasis are largely unknown.

Head and neck squamous cell carcinoma (HNSCC) is one of the leading causes of cancer deaths worldwide[19]. Intratumoral hypoxia is considered to be one of the main factors contributing to progression, metastasis and treatment resistance of HNSCC[20,21]. We recently demonstrated that direct regulation of *TWIST1*, a master regulator of mesoderm development[22,23], by hypoxia inducible factor-1 (HIF-1) promotes metastasis. Co-overexpression of HIF-1α, Twist1 and Snail in HNSCC correlates with the worst prognosis[24]. Furthermore, a previous study identified a subpopulation of cells in HNSCC with stem-like properties that were highly tumorigenic and co-expressed *CD44* and *BMI1* (ref. 17). Owing to the critical role of hypoxia in maintaining self-renewal[25], we hypothesized that the EMT regulators activated by hypoxia could induce the expression of stemness genes, resulting in promotion of EMT and tumour-initiating capability. In this report, we demonstrate the direct regulation of *BMI1* by Twist1, and the functional interdependence between Twist1 and Bmi1 in promoting EMT and the tumour-initiating capability of head and neck cancer cells.

[1]Institute of Clinical Medicine, National Yang-Ming University, No.155, Sec.2, Li-Nong Street, Peitou, Taipei 112, Taiwan. [2]Institute of Biotechnology in Medicine, National Yang-Ming University, No.155, Sec.2, Li-Nong Street, Peitou, Taipei 112, Taiwan. [3]Division of Hematology-Oncology, Department of Medicine, Taipei Veterans General Hospital, Taipei 112, Taiwan. [4]Genomic Research Center, Taipei Veterans General Hospital, Taipei 112, Taiwan. [5]Institute of Microbiology & Immunology, No.155, Sec.2, Li-Nong Street, Peitou, Taipei 112, Taiwan. [10]Taiwan Advance Biopharm, Inc, Xizhi City, Taipei County 221, Taiwan. [7]Department of Dentistry, Taipei Veterans General Hospital, Taipei 112, Taiwan. [8]Department of Otolaryngology, Taipei Veterans General Hospital, Taipei 112, Taiwan. [9]Department of Medical Research & Education, Taipei Veterans General Hospital, Taipei 112, Taiwan. [10]Institute of Biochemistry & Molecular Biology, National Yang-Ming University, No. 155, Sec. 2, Li-Nong Street, Peitou District, Taipei City 112, Taiwan.
[11]These authors contributed equally to this work.
[12]Correspondence should be addressed to: M.H.Y. and K.J.W. (e-mail: mhyang2@vghtpe.gov.tw and kjwu2@ym.edu.tw)

Received 01 December 2009; accepted 04 August 2010; published online 05 September 2010; DOI: 10.1038/ncb2099

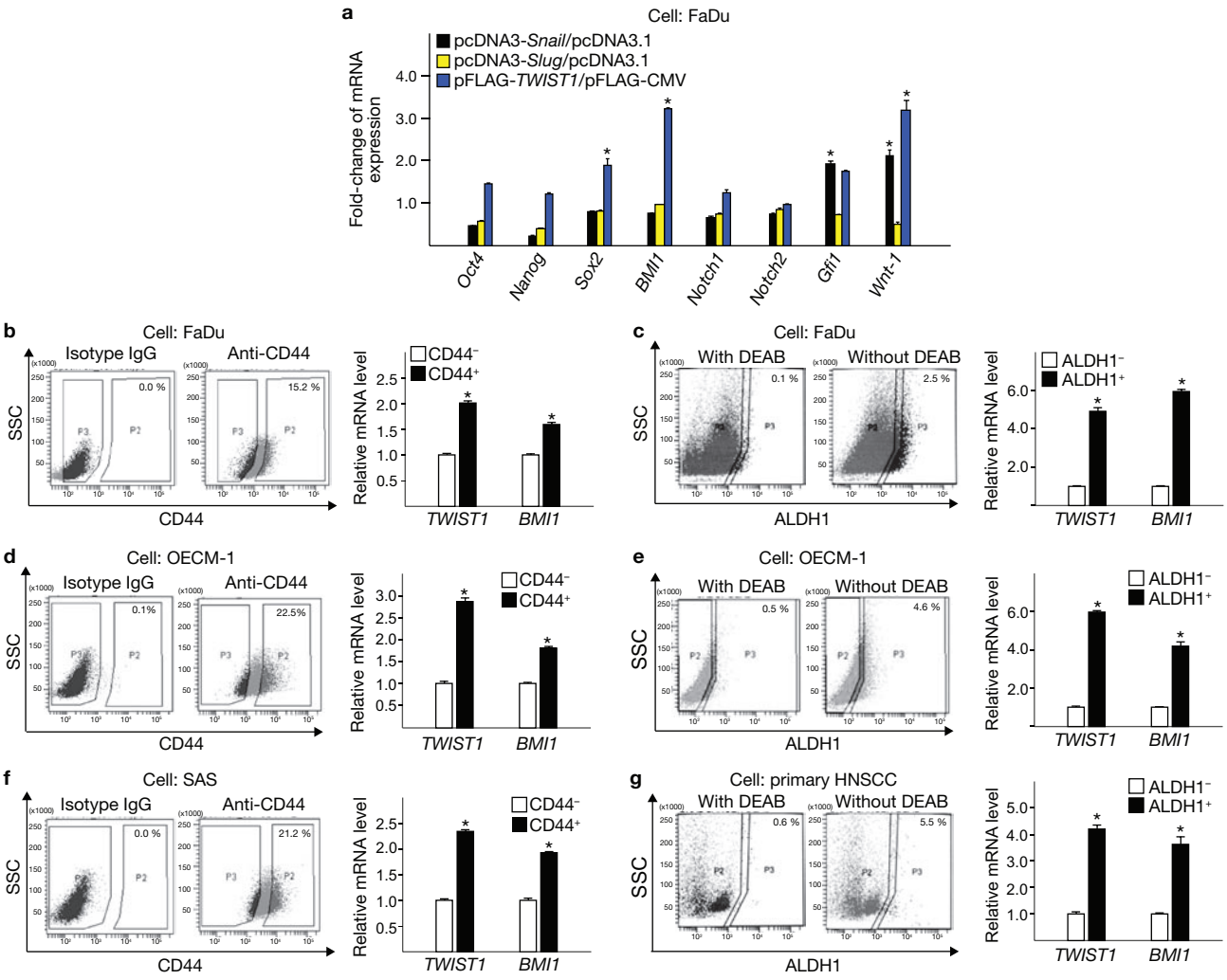

Figure 1 Overexpression of *TWIST1* upregulates *BMI1* expression, and HNSCC cells expressing putative tumour-initiating cell markers overexpress *TWIST1* and *BMI1*. (**a**) Fold-change in mRNA levels of different stemness-related genes in FaDu cells transfected with pcDNA3-*Snail*, pcDNA3-*Slug* or pFLAG-*TWIST1*. Fold-change in mRNA expression induced by each vector was calculated by normalization to the control (transfection of an empty vector; pcDNA3.1 or pFLAG-CMV, as indicated) . Data represent means ± s.e.m. ($n = 3$). Asterisk indicates $P < 0.001$, compared with cells transfected with expression and control vectors (Student's *t*-test). (**b–g**) Left, separation of cells expressing CD44 (CD44⁺; **b**, **d**, **f**) or ALDH1 (ALDH1⁺; **c**, **e**, **g**) from populations of the indicated cell lines by FACS (fluorescence-activated cell sorting). Cells were treated with FITC-conjugated antibody specific to CD44 or ALDEFLUOR reagent. Flow cytometry plots indicate side scatter (SSC) versus intensity of FITC fluorescence. P2 and P3 indicate the gated regions in flow cytometric analysis. P2: CD44⁺ in **b**, **d** and **f**; P3: ALDH1⁺ in **c**, **e** and **g**. The percentage of CD44⁺ or ALDH1⁺ cells are indicated in each panel. Cells treated with immunoglobulin G (IgG; **b**, **d**, **f**) or DEAB (diethylaminobenzaldehyde, an ALDH1 inhibitor; **c**, **e**, **g**) are negative controls. Right: Fold-change in levels of *TWIST1* and *BMI1* mRNA in CD44⁺ versus CD44⁻ cells (**b**, **d**, **f**) or ALDH1⁺ versus ALDH1⁻ cells (**c**, **e**, **g**). Data represent means ± s.e.m. ($n = 3$). Asterisks indicate $P < 0.001$, compared with controls (Student's *t*-test).

RESULTS

Direct regulation of BMI1 by Twist1.

As EMT was shown to generate cells with stem-like properties[2,3], we screened the change in expression levels of stemness-related genes *Oct-4* (*POU5F1*), *NANOG*, *GFI1*, *BMI1*, *SOX2*, *NOTCH1*, *NOTCH2* and *WNT1* in three HNSCC cell lines (FaDu, OECM-1 and SAS) overexpressing different EMT regulators (*TWIST1*, *Snail* and *Slug*). Overexpression of the EMT regulators upregulated different stemness genes, but the polycomb group gene, *BMI1*, was consistently upregulated by *TWIST1* overexpression in all three HNSCC cell lines (Fig. 1a and Supplementary Information, Fig. S1a). In addition, both *TWIST1* and *BMI1* were upregulated in HNSCC cell lines and tumour samples sorted by the putative markers for HNSCC tumour-initiating cells, CD44 and aldehyde dehydrogenase 1 (ALDH1)[17,26] (Fig. 1b–g). This suggested that *BMI1* expression may be regulated by Twist1. To confirm this, FaDu and OECM-1 cells that overexpress *TWIST1* were generated . In addition to the induction of EMT (that is, downregulation of E-cadherin and upregulation of N-cadherin), overexpression of *TWIST1* increased Bmi1 mRNA and protein expression and decreased the mRNA level of *p16INK4a* (Fig. 2a). Ectopic expression of *TWIST1* in primary HNSCC cells also upregulated *BMI1* expression and repressed *E-cadherin* and *p16INK4a* irrespective of the endogenous *TWIST1* levels (Supplementary Information, Fig. S1b). As we previously found that *TWIST1* is activated by HIF-1α[24], we tested whether Bmi1 is activated under hypoxic conditions or by *HIF-1α* overexpression. Both hypoxia and constitutive expression of a *HIF-1α*(ΔODD) mutant (with

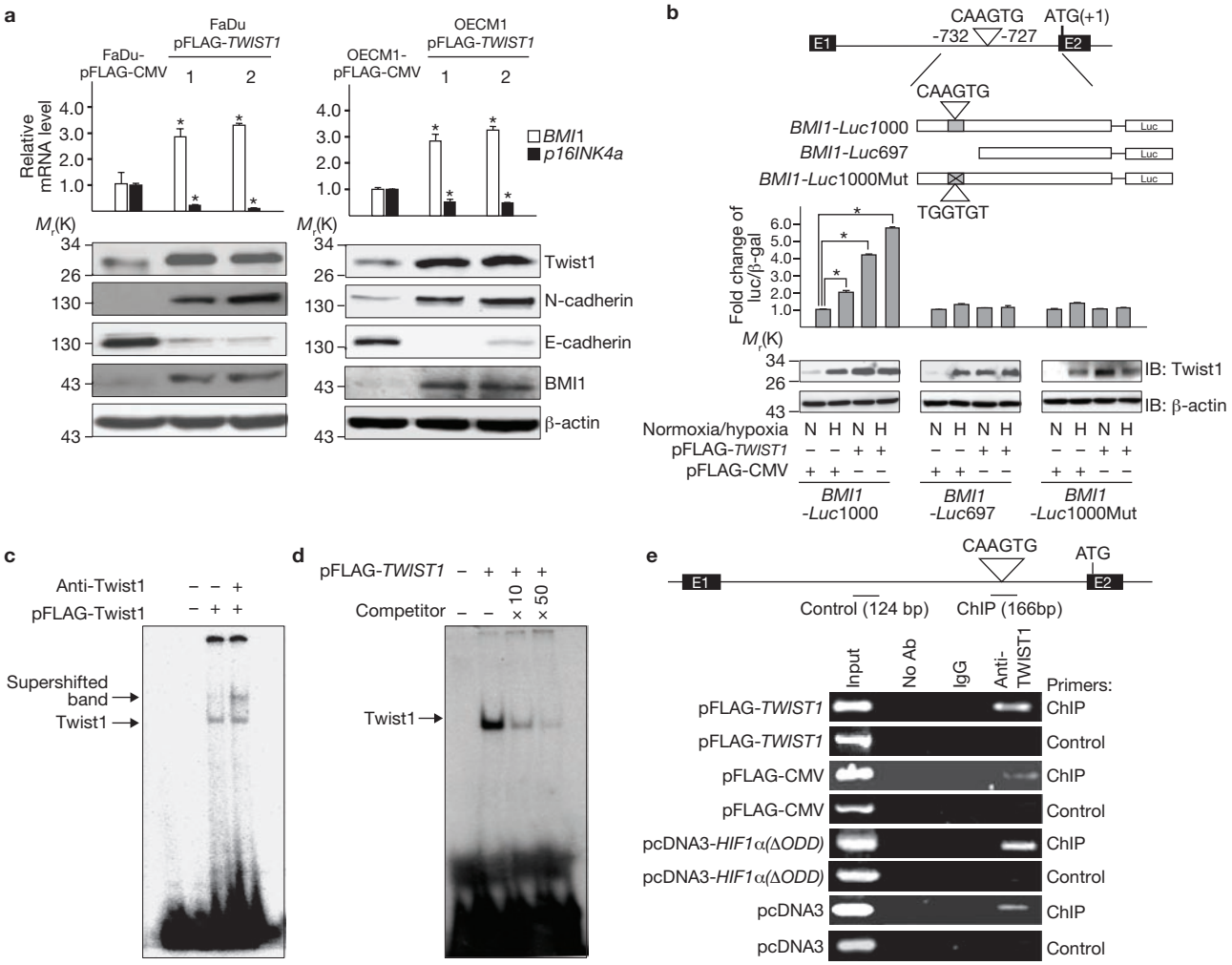

Figure 2 *BMI1* expression is directly regulated by Twist1. (**a**) Fold-change in mRNA levels of *BMI1* and *p16INK4a* (top) and western blot of indicated proteins (bottom) in FaDu cells (left) or OECM1 cells (right) transfected with the indicated vectors. Data represent means ± s.e.m. ($n = 3$) and fold-change is calculated relative to expression level of mRNA in control cells. Two independent stable clones are shown, as indicated. Asterisk indicates $P < 0.001$ (Student's *t*-test), compared with controls. β-actin was used as a loading control. (**b**) Top: schematic representation of the regulatory region of the *BMI1* gene and reporter constructs used in transfection assays. The luciferase reporter constructs were made with the wild-type *BMI1* regulatory region (*BMI1–Luc*1000), a *BMI1* regulatory region with the E-Box deleted (*BMI1–Luc*697) or a *BMI1* regulatory region with the indicated base substitutions in the E-box (*BMI1–Luc*1000Mut). E1, exon 1; E2, exon 2. Bottom: promoter-activity assay. HEK-293T cells were co-transfected with a promoter construct and the indicated vector, under normoxic or hypoxic conditions. All cells were co-transfected with a plasmid expressing *βGal* and luciferase activity values were normalized to β-galactosidase activity. For each promoter, all values are standardized to the luciferase activity of the control; asterisk indicates $P < 0.001$ (Student's *t*-test), compared with control cells. Data represent means ± s.e.m. ($n = 3$). Western blot indicates the levels of Twist1. (**c**) EMSA and supershift assay. Nuclear extracts from HEK-293T cells transfected with the indicated vectors were incubated with α^{32}P-labelled dCTP probe containing the E-box from the *BMI1* regulatory region. Addition of the anti-Twist1 antibody resulted in the supershifted band. No protein extract was added to lane 1. (**d**) EMSA and competition assay. Nuclear extracts from HEK-293T cells transfected with the indicated vectors were incubated with α^{32}P-dCTP-labelled probe from the *BMI1* regulatory region containing a Twist1-binding site. Unlabelled oligonucleotides were added at concentrations tenfold (lane 3) or 50-fold (lane 4) greater than the concentration of labelled probe. (**e**) ChIP assay of FaDu cells transfected with the indicated vectors. Schematic representation of the ChIP and control primers is shown at the top. Uncropped images of blots are shown in Supplementary Information, Fig. S8.

deletion of the oxygen degradation domain that functions in a normoxic environment[27]) induced EMT, upregulated *BMI1* expression and inhibited *p16INK4a* expression (Supplementary Information, Figs S1c, d and S2a, b).

To determine the direct regulation of *BMI1* by Twist1, we identified the putative Twist1-binding site (E-box) in intron 1 of the *BMI1* gene and generated a reporter construct. Transient transfection assays showed a fourfold increase in *BMI1* promoter activity after co-transfection with a *TWIST1* expression vector. Hypoxia augmented the *BMI1* promoter activity, and in hypoxic cells transfected with *TWIST1* there was additional activation to approximately sixfold that of control cells under normoxic conditions. Deletion or mutation of the Twist1-binding site eliminated the activation (Fig. 2b). Electrophoretic mobility shift assays (EMSA) contained a Twist1-binding band after incubation of nuclear extracts from *TWIST1*-overexpressing cells with labelled oligonucleotides containing an E-box from the *BMI1* regulatory region, and a supershifted band was seen after addition of an anti-Twist1-specific antibody to the mixture (Fig. 2c). Addition of excess amounts

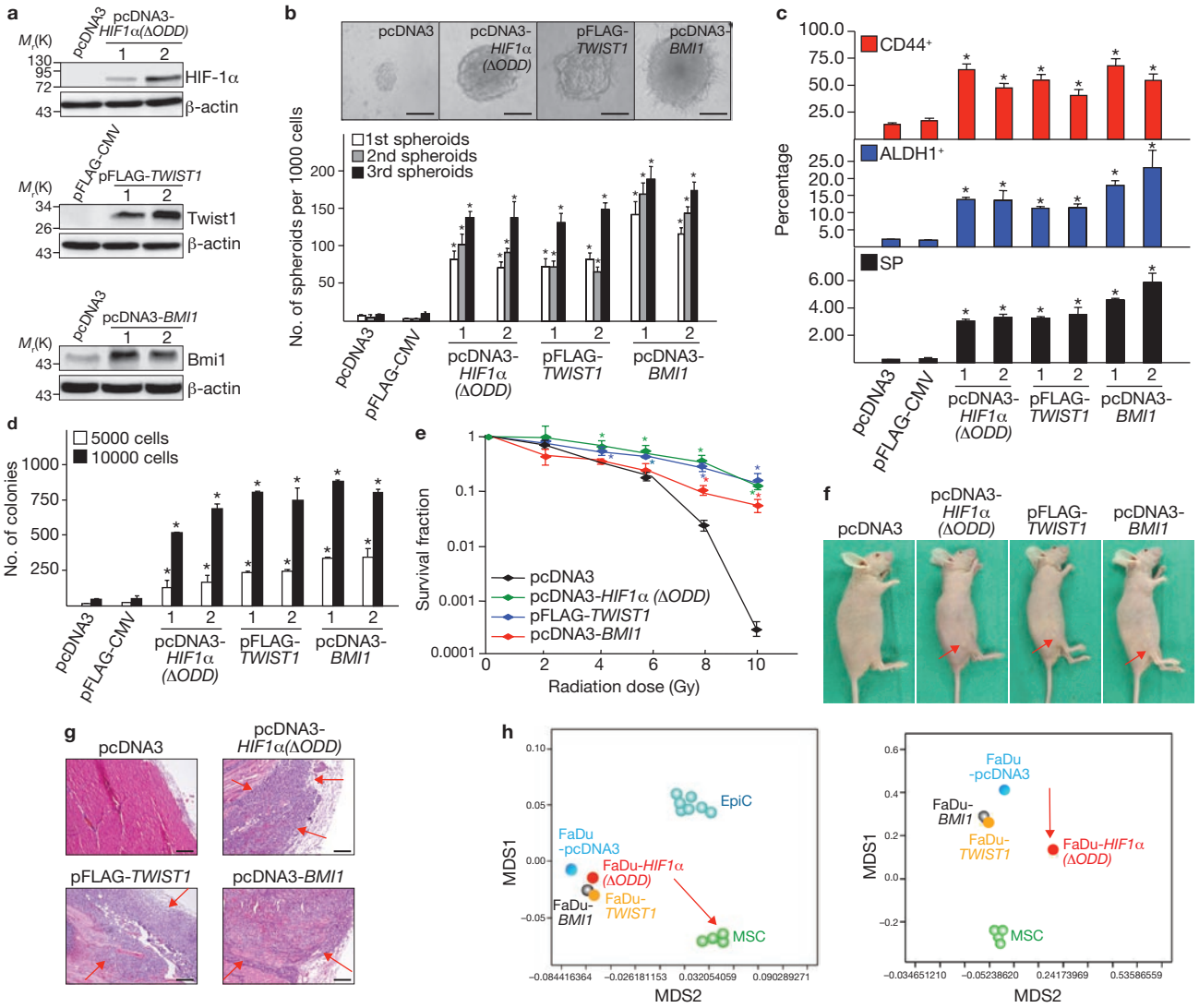

Figure 3 Overexpression of *HIF-1α*, *TWIST1* or *BMI1* promotes tumour-initiating capability of FaDu cells. (**a**) Western blot analysis of FaDu cells overexpressing *HIF-1α*, *TWIST1* and *BMI1*, compared with respective control cells. Two independent stable clones are shown. (**b**) Representative images (top) and quantification (bottom) of spheroid formation in FaDu cells transfected with the indicated vectors. Scale bars, 100 μm. Data represent means ± s.e.m. ($n = 3$) and two independent stable clones are represented, as indicated. Asterisk indicates $P < 0.001$, compared with control cells (Student's *t*-test). (**c**) Percentage of FaDu cells transfected with the indicated vectors that are CD44-positive, ALDH1-positive, or side population. Data represent means ± s.e.m. ($n = 3$) and two independent stable clones are shown, as indicated. Asterisk indicates $P < 0.001$, compared with control cells (Student's *t*-test). (**d**) Soft-agar colony formation assay of FaDu cells transfected with the indicated vectors. Colony formation was assessed from a population of either 5,000 or 10,000 cells. Data represent means ± s.e.m. and two independent stable clones are shown, as indicated ($n = 3$). Asterisk indicates $P < 0.001$, compared with controls (Student's *t*-test). (**e**) Survival fraction of FaDu cells transfected with the indicated vectors, after irradiation treatment. Data represent means ± s.e.m. ($n = 3$). Asterisks indicate $P < 0.001$, compared with FaDu cells transfected with pcDNA3 (Student's *t*-test). (**f**) Representative images of nude mice that received subcutaneous injections of FaDu cells transfected with the indicated vectors. Red arrows indicate the formation of xenotransplanted tumour. Cell dose: 1×10^3 cells per mouse. (**g**) Histological examination of the implanted sites of the mice shown in **f** by haematoxylin and eosin stains. Red arrows indicate the subcutaneous colonization and muscle infiltration of tumour cells. Scale bars, 500 μm. (**h**) Left: a multidimensional scaling (MDS) plot analysing the whole transcriptome of FaDu cells, transfected with transfected with the indicated vectors, compared with epithelial (EpiC) and mesenchymal stem cells (MSCs). Right: a MDS plot where genes that were expressed at a similar level in both MSCs and FaDu-pcDNA3 cells were removed and the differentially expressed genes ($q < 0.01$) were then analysed in FaDu cells transfected with the indicated vectors. The arrow indicates the transcriptome-drifting direction. Uncropped images of blots are shown in Supplementary Information, Fig. S8.

of unlabelled oligonucleotides containing an E-box outcompeted and abolished the binding activity of Twist1 (Fig. 2d). Chromatin immunoprecipitation (ChIP) confirmed the direct binding of Twist1 to the *BMI1* regulatory region (Fig. 2e). These results demonstrate that Twist1 directly activates *BMI1* transcription by binding to the E-box in intron 1 of the *BMI1* gene.

Enhanced tumour-initiating capability in HNSCC cells that overexpress HIF-1α, TWIST1 or BMI1.

We next investigated the impact of HIF-1α, Twist1 or Bmi1 on the tumour-initiating capability of HNSCC cells. In FaDu cells, there was a significant increase in formation of spheroids, which indicates that the cells are capable of initiating tumours[28], when *HIF-1α*, *TWIST1* or *BMI1* were

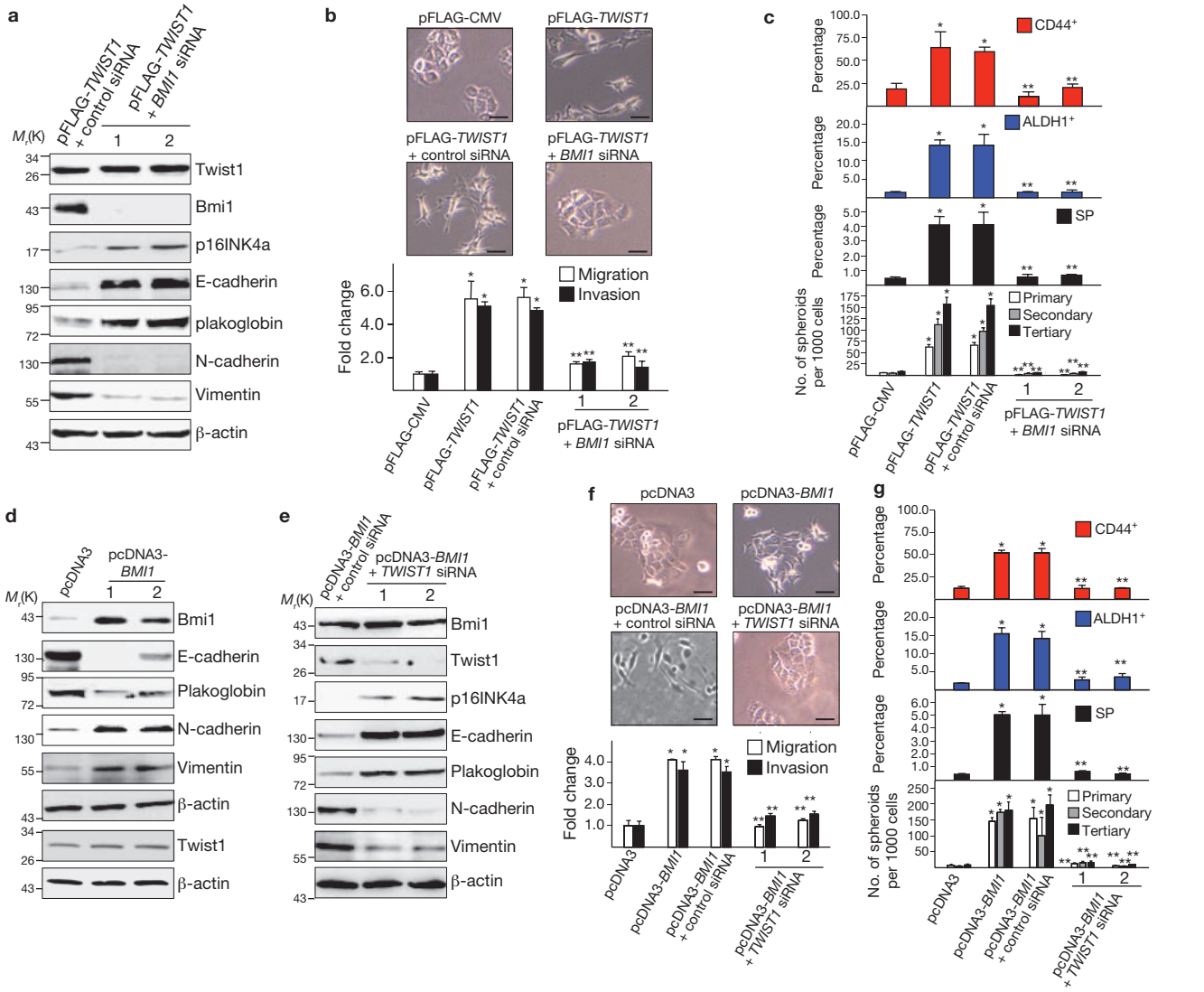

Figure 4 Twist1 and Bmi1 are mutually essential for maintaining EMT and tumour-initiating capability, and overexpression of *BMI1* induces EMT. (**a**) Western blot analysis of FaDu cells overexpressing *TWIST1* and then transfected with siRNA against Bmi1, or an siRNA with a scrambled sequence (control). Two independent stable clones are shown, as indicated. (**b**) Phase-contrast microscopy images (top) and migration and invasion ability (bottom) of FaDu cells transfected with empty control vector (pFLAG-CMV), overexpressing *TWIST1*, or overexpressing *TWIST1* and then transfected with control or *BMI1* siRNA. Scale bars, 50 μm. Data represent means ± s.e.m. ($n = 3$). Asterisks indicates $P < 0.001$, compared with FaDu cells transfected with empty pFLAG-CMV vector and double asterisks indicate $P < 0.001$, compared with cells transfected with control siRNA (Student's *t*-test). Two independent stable clones are shown, as indicated. (**c**) Percentage of CD44-positive, ALDH1-positive, and side-population (SP) cells and the spheroid-forming capacity of FaDu cells, transfected with the indicated vectors and siRNA. Data represent means ± s.e.m. ($n = 3$). Asterisks indicate $P < 0.001$, compared with cells transfected with empty pFLAG-CMV vector and double-asterisks indicate $P < 0.001$, compared with cells transfected with control siRNA (Student's *t*-test). (**d**) Western blot analysis of FaDu cells transfected with empty control vector or overexpressing *BMI1*. Two independent stable clones are shown, as indicated. (**e**) Western blot analysis of FaDu cells overexpressing *BMI1* and transfected with either control siRNA or *TWIST1* siRNA. Two independent stable clones are shown, as indicated. (**f**) Phase-contrast microscopy images (top) and migration and invasion ability (bottom) of FaDu cells transfected with the indicated vectors and siRNA. Data represent means ± s.e.m. ($n = 3$). Asterisks indicate $P < 0.001$, compared with control. Double-asterisks indicate $P < 0.001$, compared with cells transfected with control siRNA (Student's *t*-test). Two independent stable clones are shown, as indicated. (**g**) Percentage of CD44-positive, ALDH1-positive and side-population (SP) cells and the spheroid-forming capacity of FaDu cells, transfected with the indicated vectors and siRNA. Asterisks indicates $P < 0.001$, compared with cells transfected with empty control vector. Double-asterisks indicate $P < 0.001$, compared with cells transfected with control siRNA ($n = 3$). Uncropped images of blots are shown in Supplementary Information, Fig. S8.

were overexpressed (Fig. 3a, b). A significant proportion of *HIF-1α*-, *TWIST1*- or *BMI1*-overexpressing cells bore putative markers of tumour-initiation (that is, they were CD44- or ALDH1-positive or were side-population cells), compared with control cells (Fig. 3c and Supplementary Information Fig. S3a–c). Overexpression of *HIF-1α*, *TWIST1* or *BMI1* increased anchorage-independent growth and resistance to irradiation (Fig. 3d, e). Similar results were found in OECM-1 cells overexpressing *HIF-1α*, *TWIST1* or *BMI1* (Supplementary Information, Fig. S4a–d). Importantly, FaDu cells overexpressing *HIF1α*(ΔODD), *TWIST1* or *BMI1* showed an enhanced *in vivo* tumour formation ability in nude mice, especially in mice receiving injections of lower cellular doses (Fig. 3f, g and Supplementary Information, Table S1). The tumour-initiating capability

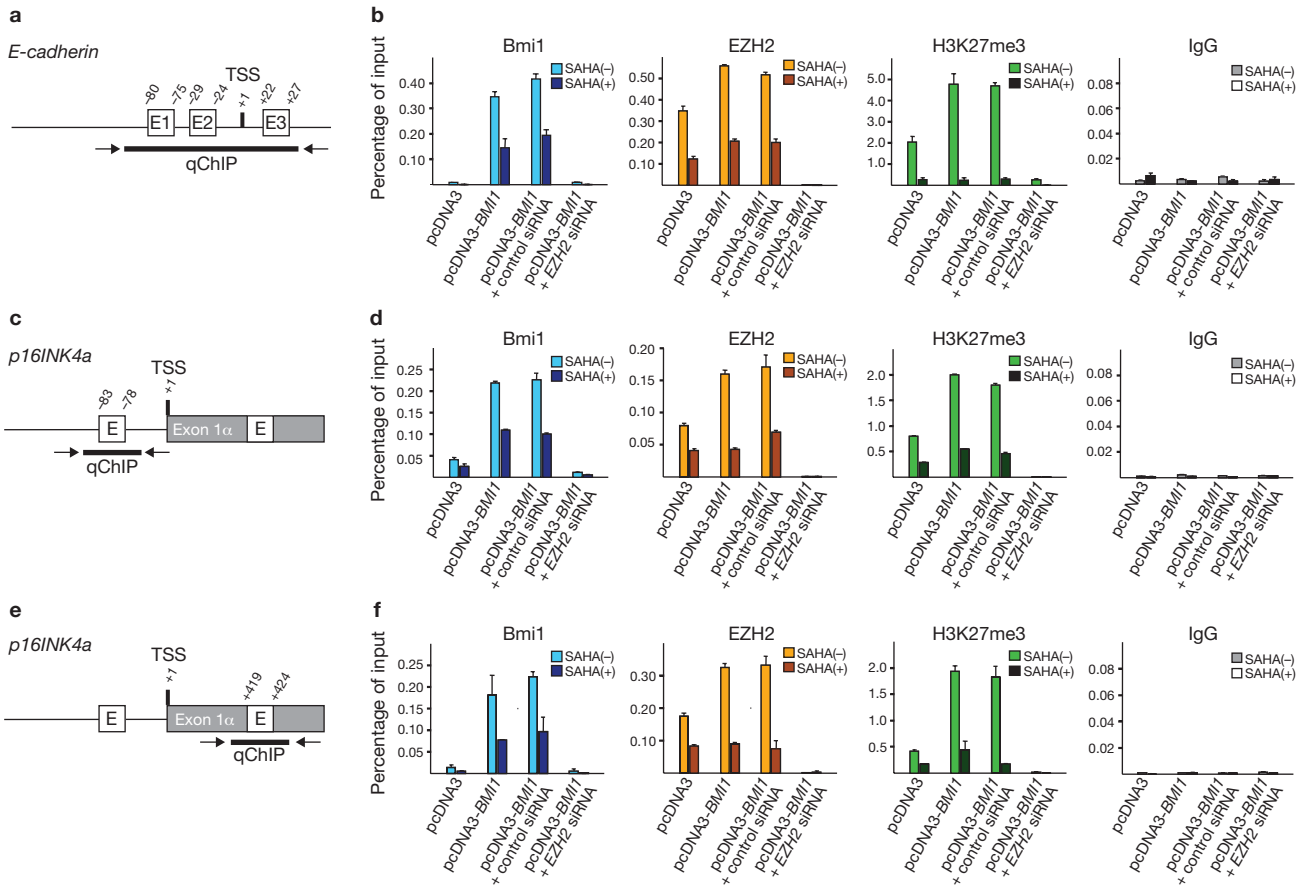

Figure 5 The Bmi1-containing polycomb repressive complex binds to the *E-cadherin* promoter, *p16INK4a* promoter and exon 1α. (**a**) Schematic representation of the promoter region of *E-cadherin*. E1, E2 and E3 indicate the location of E-boxes. The arrows indicate the fragment amplified in qChIP analysis. TSS; transcription start site. (**b**) qChIP assay of the *E-cadherin* promoter region in FaDu cells transfected with empty pcDNA3 vector, overexpressing BMI1, or overexpressing BMI1 and then transfected with either control or EZH2 siRNA, with or without suberoylanilide hydroxamic acid (SAHA) treatment. Data represent means ± s.e.m. ($n = 3$). The antibodies used in qChIP are indicated at the top of each panel; IgG was used as a control. (**c**) Schematic representation of the *p16INK4a* promoter. E indicates the location of E-boxes. The arrows indicate the fragment amplified in qChIP analysis. (**d**) qChIP assay of the *p16INK4a* promoter region in cells transfected as in **b.** Data represent means ± s.e.m. ($n = 3$). (**e**) Schematic representation of the *p16INK4a* exon 1α. E indicates the location of E-boxes. The arrows indicate the amplified fragment in qChIP analysis. (**f**) qChIP assay of the *p16INK4a* exon 1α in FaDu cells transfected as in **b**. Data represent means ± s.e.m. ($n = 3$). The binding activity of each protein is given as percentage of total input.

(incidence of tumour formation per cell dose) of control FaDu cells transfected with pcDNA3 vector was 4×10^{-6}, compared with 6×10^{-4} in FaDu cells overexpressing *HIF1α*(ΔODD), *TWIST1* or *BMI1*, which is a 150-fold enhancement. These results demonstrate an enhanced tumour-initiating capability in HNSCC cells overexpressing *HIF-1α*, *TWIST1* or *BMI1*.

Twist1 and Bmi1 are mutually essential in inducing EMT and promoting tumour-initiating capability.

Next, we investigated the impact of *HIF-1α*, *TWIST1* or *BMI1* expression on transcriptome reprogramming of cancer cells. Overexpression of *HIF-1α*, *TWIST1* or *BMI1* in FaDu cells caused a transcriptome drift to a mesenchymal stem cell-like status. Surprisingly, a highly overlapping transcriptome was found between FaDu cells overexpressing *TWIST1* and FaDu cells overexpressing *BMI1* (Fig. 3h and Supplementary Information, Fig. S4e). This result suggests that Twist1 and Bmi1 may act cooperatively to promote cancer dedifferentiation and metastasis. Bmi1 was knocked down to examine its role in maintaining EMT and promoting tumour-initiating capability in *TWIST1*-overexpressing cells. Knockdown of Bmi1 led to reversion of EMT and a decrease in *in vitro* migration and invasion ability (Fig. 4a, b and Supplementary Information, Fig. S2c). Bmi1 suppression also upregulated *p16INK4a* expression (Fig. 4a), reduced the percentage of CD44-positive, ALDH-positive and side-population cells, decreased spheroid-forming ability (Fig. 4c and Supplementary Information, Fig. S3d–h), and attenuated *in vivo* tumour formation (Supplementary Information, Table S2) of FaDu cells overexpressing *TWIST1*, indicating the reduction of tumour-initiating capability. We then investigated the role of the Twist1–Bmi1 pathway in HIF-1α-induced EMT and cell stemness properties. Knockdown of Bmi1 in FaDu cells overexpressing *HIF1α*(ΔODD) resulted in a reversion of EMT, attenuation of *in vitro* migration/invasion, a decrease in the proportion of cells harbouring stemness markers and inhibition of spheroid-forming ability (Supplementary Information, Figs S2b and S5a–d). Furthermore, knockdown of Twist1 in FaDu cells overexpressing *HIF1α*(ΔODD) also downregulated *BMI1* expression, reverted EMT and reduced stemness properties (Supplementary Information, Figs S2b and S5e–g).

As we had found a critical role for Bmi1 in Twist1-mediated EMT, we investigated the ability of Bmi1 to induce EMT. Overexpression of

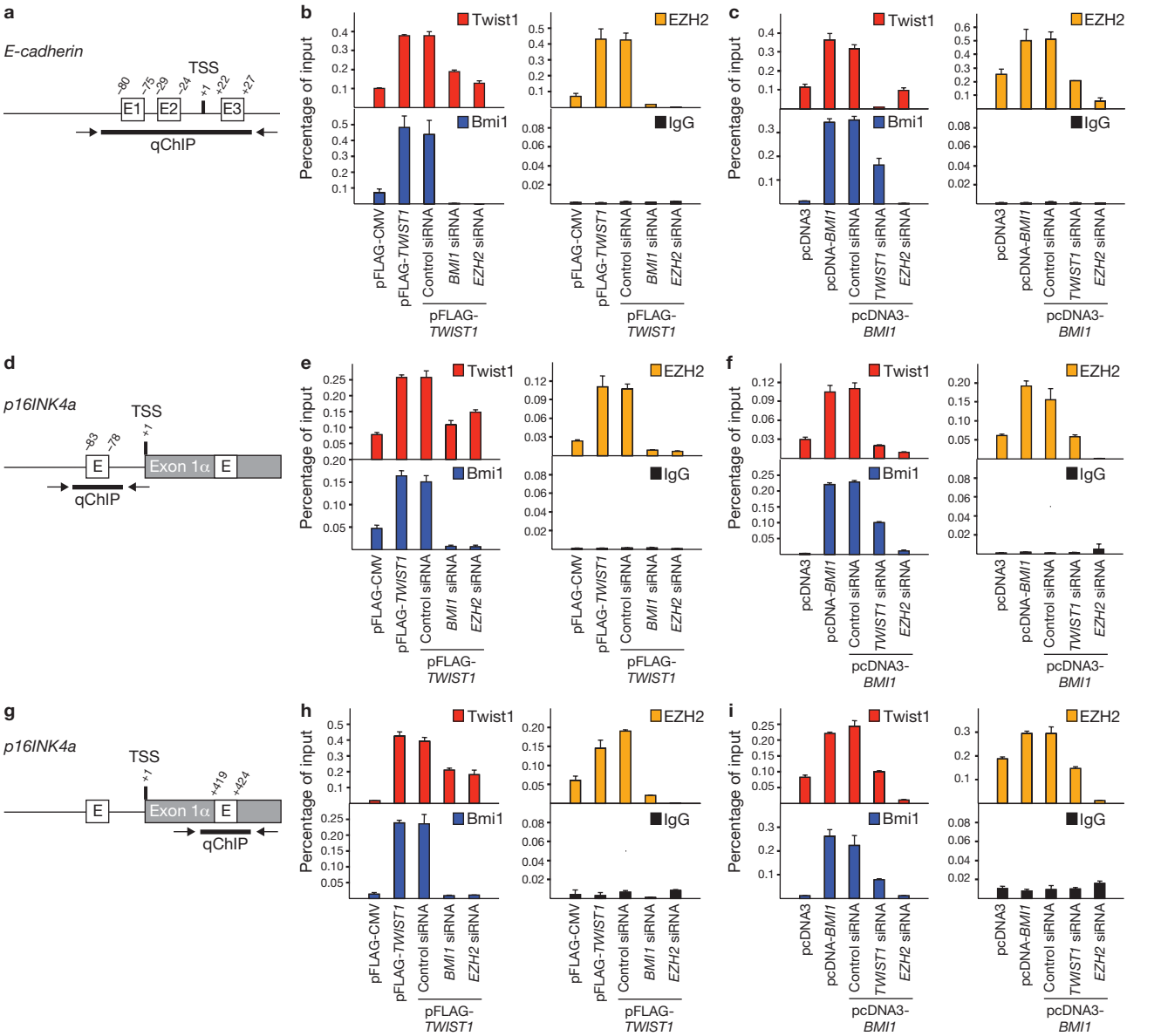

Figure 6 Co-occupancy of Twist1, Bmi1 and EZH2 on the *E-cadherin* promoter, *p16INK4a* promoter and exon 1α. (**a**) Schematic representation of the promoter region of *E-cadherin*. E1, E2 and E3 indicate the location of E-boxes. The arrows indicate the amplified fragment in quantitative chromatin immunoprecipitation (qChIP) analysis. (**b**) qChIP assay for the *E-cadherin* promoter region in FaDu cells transfected with empty pFLAG-CMV vector, overexpressing *TWIST1*, or overexpressing TWIST1 and transfected with siRNA against *BMI1*, *EZH2* or a control siRNA with a scrambled sequence. Data represent means ± s.e.m. ($n = 3$). The antibodies used in qChIP are shown in each panel, and IgG was applied as a control. The binding activity of each protein is given as percentage of total input. (**c**) qChIP assay for the *E-cadherin* promoter region in FaDu cells transfected with empty pcDNA3 vector, overexpressing *BMI1*, or overexpressing BMI1 and transfected with *TWIST1* siRNA, *EZH2* siRNA or a scrambled sequence, control siRNA. Data represent means ± s.e.m. ($n = 3$). The binding activity of each protein is given as percentage of total input. (**d**) Schematic representation of the promoter region of *p16INK4a*. (**e**) qChIP assay for the *p16INK4a* promoter region in FaDu cells transfected and processed as in **b**. Data represent means ± s.e.m. ($n = 3$). (**f**) qChIP assay for the *p16INK4a* promoter region in FaDu cells transfected and processed as in **c**. Data represent means ± s.e.m. ($n = 3$). (**g**) Schematic representation of the exon 1α of *p16INK4a*. (**h**) qChIP assay for the exon 1α of *p16INK4a* in FaDu cells transfected and processed as in **b**. Data represent means ± s.e.m. ($n = 3$). (**i**) qChIP assay for the exon 1α of *p16INK4a* in FaDu cells transfected and processed as in **c**. Data represent means ± s.e.m. ($n = 3$).

BMI1 in FaDu cells induced EMT, as characterized by downregulation of epithelial markers, upregulation of mesenchymal markers, fibroblast-like changes and an increase in migration and invasion (Fig. 4d, f and Supplementary Information, Fig. S2d). To address whether feedback regulation exists between Twist1 and Bmi1, we analysed the change of *TWIST1* expression in FaDu, OECM-1 and primary HNSCC cells after ectopic expression of *BMI1*. Overexpression of *BMI1* did not influence the mRNA and protein levels of Twist1. Furthermore, knockdown of endogenous Bmi1 in OECM-1 cells did not affect *TWIST1* expression (Supplementary Information, Fig. S5h–j). These results suggest that Twist1 is located upstream of Bmi1 and regulates its expression, and there is no feedback regulation between these two factors.

To further test the cooperative role of Twist1 and Bmi1 to promote EMT and tumour-initiating capability, Twist1-knockdown clones were

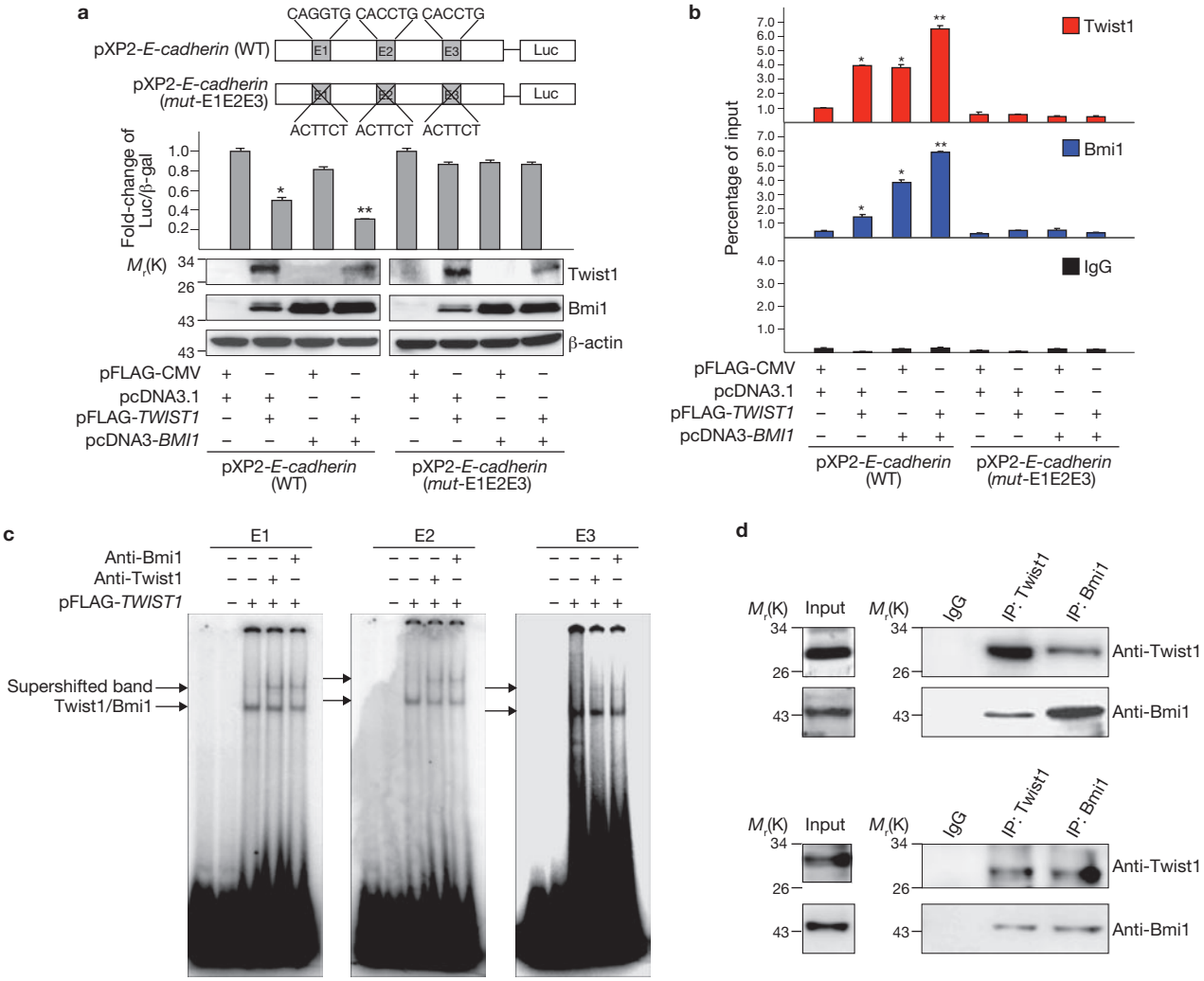

Figure 7 Twist1 and Bmi1 cooperatively repress *E-cadherin* transcription. (**a**) Top: schematic representation of the wild-type (pXP2-E-cadherin) or E-boxes-mutated (pXP2-E-cadherin(*mut*-E1E2E3)) *E-cadherin* promoter construct. E1, E2 and E3 indicate E-boxes. Bottom: promoter activity assay in HEK-293T cells under different transfections. A vector expressing β-galactosidase was co-transfected to ensure transfection efficiency and normalize luciferase activity values. For analysis of each promoter luciferase activity of the cells was normalized to the control cells transfected with the empty vectors (pcDNA3.1 and pFLAG-CMV). The protein levels of Twist1 and Bmi1 were shown to indicate their levels under different transfections. Data represent means ± s.e.m. ($n = 3$). Asterisks indicate $P < 0.001$ between cells transfected with single expression vector (pFLAG-*TWIST1* or pcDNA3-*BMI1*) and the empty vectors. Double-asterisks indicate in the same promoter analysis, $P < 0.001$ between cells transfected with pFLAG-*TWIST1*, and pFLAG-*TWIST1* and pcDNA3-*BMI1* (Student's *t*-test). (**b**) Plasmid immunoprecipitation assay of HEK-293T cells co-transfected with *E-cadherin* promoter, empty vector and/or expression vector, as indicated. The antibodies used are shown in each panel; IgG was used as a control. The binding activity of each protein is given as the percentage of total input. Data represent means ± s.e.m. ($n = 3$). Asterisk indicates $P < 0.001$ between cells transfected with single expression vector (pFLAG-*TWIST1* or pcDNA3-*BMI1*) and the empty vector. Double-asterisks (**) indicate in the same promoter analysis, $P < 0.001$ between cells transfected with pFLAG-*TWIST1*, and pFLAG-*TWIST1* and pcDNA3-*BMI1* (Student's *t*-test). (**c**) EMSA and supershift assay. Nuclear extracts from HEK-293T cells transfected with pFLAG-CMV (lane 2 of each panel) or pFLAG-*TWIST1* (lane 3–5 of each panel) were incubated with different α^{32}P-labelled dCTP oligonucleotide probes containing the different E-boxes (E1, E2 or E3) of the *E-cadherin* promoter, as indicated. Addition of anti-Twist1 or anti-Bmi1 antibody resulted in the supershifted bands. No protein extract was added to lane 1 in each panel. (**d**) Co-immunoprecipitation assays using an anti-Twist1 or an anti-Bmi1 antibody to pull down proteins from nuclear extracts of FaDu cells overexpressing *TWIST1* (top) or *BMI1* (bottom). IgG was used as a control. Uncropped images of blots are shown in Supplementary Information, Fig. S8.

generated in FaDu cells overexpressing *BMI1* . As expected, Twist1 suppression abolished the induction of EMT and tumour-initiating capability by Bmi1 (Fig. 4e–g and Supplementary Information, Figs S2d and S3i–m, and Table S2). These results indicate that Twist1 and Bmi1 are mutually essential to induce EMT and promote tumour-initiating capability in cancer cells, and both proteins have a critical role in HIF-1α-induced EMT and cell stemness properties.

Bmi1-containing PRC directly represses *E-cadherin* expression. As Bmi1 is able to induce EMT, we hypothesized that Bmi1-containing PRC could directly repress *E-cadherin* expression. To address this issue, ten pairs of primers were designed that span the promoter region of *E-cadherin* (approximately 3 kb) and quantitative ChIP (qChIP) assays were performed in FaDu cells overexpressing *BMI1*. The most significant enhancement of Bmi1 binding activity was found from –170 bp

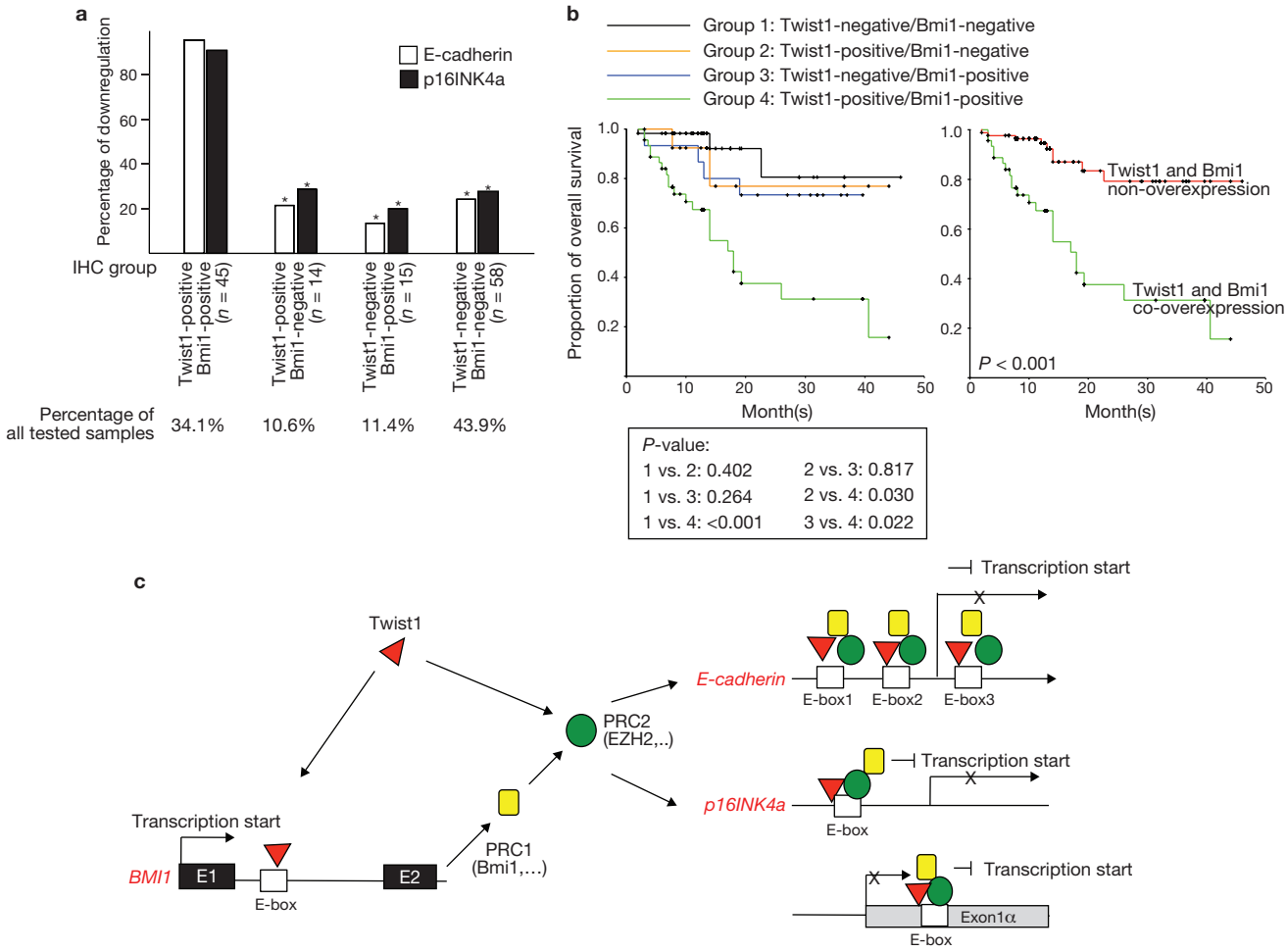

Figure 8 Clinical significance of Twist1 and Bmi1 in HNSCC patients and a proposed model of Twist1- and Bmi1-mediated suppression of E-cadherin and p16INK4a. (**a**) Percentages of cases with downregulation of E-cadherin or p16INK4a in samples with different levels of Twist1 and Bmi1, as assessed by IHC. Asterisk indicates $P < 0.01$ between the Twist1-positive/Bmi1-positive group and other groups of patients (chi-square test). (**b**) Left: comparison of the overall survival periods of patients with different levels of Twist1 and Bmi1. The *P* values of the comparison between each group are shown in the inset (log-rank test). Right: prognostic significance of overexpression of both Twist1 and Bmi1 protein in HNSCC cases. (**c**) A proposed model of Twist1- and Bmi1-mediated suppression of *E-cadherin* and *p16INK4a*. Twist1 activates the transcription of *BMI1*, and Twist1 interacts with Bmi1-containing PRC1 and PRC2 to suppress the transcription of *E-cadherin* and *p16INK4a* through binding to the E-box(es) located in the proximal promoter of *E-cadherin*, *p16INK4a* and exon 1α of *p16INK4a*. PRC; polycomb repressive complex.

to approximately + 30 bp relative to the transcription start site (+1) of the *E-cadherin* promoter (data not shown). To confirm the essential role of PRC in Bmi1-mediated *E-cadherin* repression, qChIP assays were performed in the *E-cadherin* promoter region with the highest Bmi1 binding (Fig. 5a). Increased Bmi1- and EZH2-binding, and H3K27me3 levels, were found in FaDu cells overexpressing *BMI1*, and knockdown of EZH2 decreased the levels of Bmi1- and EZH2-binding, and H3K27me3. All clones treated with suberoylanilide hydroxamic acid (SAHA), a histone deacetylase inhibitor that represses H3K27 trimethylation and PRC2 occupancy on the *E-cadherin* promoter[29], had decreased levels of Bmi1- and EZH2-binding and H3K27me3 (Fig. 5b). We also confirmed the PRC-mediated suppression of *p16INK4a*, which Bmi1 targets to regulate senescence and stem-like properties[9,10], in HNSCC cells. qChIP also showed that there is increased Bmi1- and EZH2-binding and H3K27me3 levels on the promoter and exon 1α of *p16INK4a* in FaDu cells overexpressing *BMI1*, compared with the control. Knockdown of EZH2, or treatment with SAHA, decreased Bmi1- and EZH2-binding and H3K27me3 levels (Fig. 5c–f). These results indicate that Bmi1 inhibits both *E-cadherin* and *p16INK4a* expression through a PRC-dependent mechanism.

Co-occupancy of Twist1 and Bmi1 on the regulatory regions of *E-cadherin* and *p16INK4a*.

As Twist1 and Bmi1 function cooperatively to promote EMT and tumour-initiating capability, we hypothesized that Twist1 acts with Bmi1 to repress *E-cadherin* and *p16INK4a* through a PRC-dependent mechanism. We examined the nucleotide sequences of the regions with enhanced PRC-binding (that is, the promoter of *E-cadherin* and the promoter and exon 1α of *p16INK4a*). Surprisingly, all three regions contained E-boxes (Fig. 6a, d, g), the putative Twist1-binding site, suggesting that Twist1 participates in PRC-mediated repression of *E-cadherin* and *p16INK4a*. qChIP of FaDu cells overexpressing *TWIST1* showed that there is increased binding of Twist1, Bmi1 and EZH2 to the *E-cadherin* promoter and *p16INK4a* promoter and exon 1α, compared with control cells. Binding of Twist1 to these regions was abrogated when either Bmi1 or EZH2 was knocked down (Fig. 6b, e, h). Similarly, knockdown

of endogenous Twist1 or EZH2 in FaDu cells overexpressing *BMI1* decreased binding by Twist1 and EZH2, as well as by Bmi1 (Fig. 6c, f, i). These results suggest that Twist1 and PRC containing Bmi1 simultaneously bind to the regulatory regions of *E-cadherin* and *p16INK4a*.

Cooperative repression of *E-cadherin* by Twist1 and Bmi1.

We further investigated the correlation between Twist1 and Bmi1 simultaneously binding to, and repressing, the *E-cadherin* promoter. A promoter-activity assay showed that Twist1 represses wild-type *E-cadherin* promoter activity. Mutation of each E-box reduced the extent of Twist1-mediated repression, and mutation of all three E-boxes abrogated repression by Twist1. qChIP confirmed the binding of Twist1 to the *E-cadherin* promoter (Supplementary Information, Fig. S6a,b), suggesting the direct regulation of *E-cadherin* by the Twist1-containing complex.

We next examined the collaborative effect of Twist1 and Bmi1 in *E-cadherin* repression. Promoter activity was analysed by transfection of *TWIST1* and/or *BMI1* expression vector(s) together with an *E-cadherin* promoter-containing reporter construct into HEK-293T, FaDu or OECM-1 cells. Overexpression of *TWIST1* suppressed *E-cadherin* promoter activity in all of the cell lines. Ectopic expression of *BMI1* resulted in a lesser degree of *E-cadherin* suppression in HEK-293T cells, compared with a higher degree of suppression in FaDu and OECM-1 cells. Co-expression of both proteins augmented the repression significantly in all the cell lines. Mutation of E-boxes abolished the repression by Twist1 and/or Bmi1 (Fig. 7a and Supplementary Information, Fig. S6c, d). Consistently, similar results were obtained by transfecting FaDu or OECM-1 cells stably expressing *TWIST1* or *BMI1* with the reporter constructs containing the wild-type or E-box-mutated *E-cadherin* promoter (Supplementary Information, Fig. S6e, f).

We aimed to confirm the direct co-regulation of *E-cadherin* by Twist1 and Bmi1. A plasmid immunoprecipitation assay showed that overexpression of *TWIST1* or *BMI1* in HEK-293T cells enhanced their binding to the ectopic *E-cadherin* promoter, and co-expression of both proteins augmented the binding activity (Fig. 7b). Mutations of E-boxes abolished the binding of Twist1 and/or Bmi1 to the ectopic *E-cadherin* promoter (Fig. 7b). EMSA demonstrated that the protein complex binding to the E-boxes of *E-cadherin* promoter contained both Twist1 and Bmi1 as there was a supershifted band after addition of either the anti-Twist1 or anti-Bmi1 antibody to a reaction mixture that contained the nuclear extracts from *TWIST1*-overexpressing cells transfected with a probe containing one of the three *E-cadherin* promoter E-boxes (Fig. 7c). Co-immunoprecipitation further confirmed the physical association between Twist1 and Bmi1. In *TWIST1*-overexpressing cells, both Bmi1 and Twist1 proteins were present in the immunoprecipitates obtained with the anti-Twist1 or anti-Bmi1 antibody. The same finding was also observed in *BMI1*-overexpressing cells (Fig. 7d). These results demonstrate the cooperative repression of *E-cadherin* by Twist1 and Bmi1, which depends on the presence and integrity of Twist1-binding sites.

Overexpression of both Twist1 and Bmi1 suppresses *E-cadherin* and *p16INK4a* and is associated with the worst outcome in HNSCC patients.

To confirm the findings derived from *in vitro* and animal experiments, we analysed the levels of Twist1, Bmi1, E-cadherin and p16INK4a by immunohistochemistry (IHC) in samples from 132 HNSCC cases. The characteristics of these cases are given (Supplementary Information, Table S3), and representative IHC results are shown in Supplementary Information, Figure S7. The IHC grading of Twist1 was closely associated with Bmi1 ($P < 0.001$; Supplementary Information, Table S4). Higher levels of Twist1 and Bmi1 were significantly associated with downregulation of both E-cadherin and p16INK4a. A higher level of either Twist1 or Bmi1 alone was not associated with E-cadherin or p16INK4a repression, and lower levels of Twist1 and Bmi1 in tumour cells significantly correlated with a reduction in downregulation of E-cadherin and p16INK4a (Fig. 8a). Further analysis showed that in Twist1-positive (that is, IHC 3+)/Bmi1-negative (that is, IHC 0 to approximately 2+) cases, E-cadherin and p16INK4a were downregulated only if endogenous Bmi1 was present (that is, IHC 2+; data not shown). Higher levels of both Twist1 and Bmi1 seemed to be correlated with a higher tumour grade, although the statistical significance was not reached ($P = 0.166$; Supplementary Information, Table S5). Higher levels of both Twist1 and Bmi1 was associated with the worst survival rate, compared with other groups of patients (Fig. 8b). In summary, our results demonstrate the correlation between higher levels of Twist1 and Bmi1 and *E-cadherin*–*p16INK4a* repression, which was associated with the worse outcome in HNSCC patients.

DISCUSSION

Several mechanisms, including transcriptional repression and promoter hypermethylation, have been shown to repress *E-cadherin* expression and induce EMT[1,30]. Emerging evidence has also highlighted the role of chromatin modification in *E-cadherin* repression. Snail interacts with HDAC1–HDAC2, AJUBA–PRMT5 or PRC2, to repress *E-cadherin* expression[31–33]. However, the role of Twist1 in chromatin modification has not been thoroughly explored. Here, we demonstrate the direct regulation of the chromatin modifier *BMI1* by Twist1. Bmi1 and Twist1 act cooperatively to repress *E-cadherin*. Furthermore, *in vitro* and *in vivo* assays confirm the interdependence between Twist1 and Bmi1 in promoting EMT and the tumour-initiating capability of cancer cells. This discovery not only provides a novel mechanism of EMT induction through chromatin modification, but also elucidates the signalling pathways involved in initiating the tumour capability of cells undergoing EMT. A recent report showed that Bmi1 is induced by another EMT regulator Zeb1 through regulation of the microRNA (miR)-200 family in pancreatic cancer cells[34]. Together with our findings, it indicates that Bmi1 may be a fundamental component of EMT-induced stemness of cancer cells. Bmi1 may be regulated by different regulators among different types of cancers, such as Twist1 in HNSCC and the Zeb1–miR-200 family in pancreatic cancers.

The prognostic impact of Twist1 and Bmi1 has been demonstrated in different cancers including HNSCC[24,35–37], but their relationship has not been thoroughly explored. Here, we show the cooperative role between Twist1 and Bmi1 in HNSCC, as only co-overexpression of both proteins correlates with downregulation of *E-cadherin* and *p16INK4a* and the worst prognosis. Patients that tested positive for either Twist1 or Bmi1 alone had a better prognosis than those with overexpression of both proteins. This observation further strengthens our discovery that in HNSCC, Twist1 and Bmi1 interdependently promote EMT and stemness, resulting in an extremely poor prognosis for patients. In our study, Twist1 failed to fully activate Bmi1 in approximately 10% of cases, which may be because of the heterogeneity in tumour samples. Subgroup analysis of the Twist1-positive/Bmi1-negative cases highlights that the

presence of endogenous Bmi1 or partial activation of Bmi1 by Twist1 (IHC 2+ in this study) also partly contributes to target-gene repression in HNSCC cells with higher levels of Twist1, which is consistent with our finding from *in vitro* assays.

Tumour hypoxia has been linked to an aggressive phenotype and correlates with lower survival for cancer patients. HIF-1 directly or indirectly regulates the expression of EMT regulators[1,24,35]. Accumulating evidence also suggests that hypoxia is important for maintenance of stem cells[25]. In this study, we demonstrate that hypoxia-induced Twist1 activated *BMI1* expression and cooperatively acted with Bmi1. Knockdown of either Twist1 or Bmi1 reverted EMT and attenuated cell stemness properties induced by hypoxia. These results provide a critical pathway for hypoxia-induced EMT and stemness. Previous research has demonstrated that HIF-1α activates the Notch pathway[38], the critical signals mediating both EMT and stemness[39,40]. Our results suggest that HIF-1α promotes EMT and stemness in cancer cells through a different signal pathway, that is through Twist1–Bmi1.

In conclusion, our findings provide mechanistic insight into the induction of EMT and tumour-initiating capability by an EMT regulator (Twist1) and a PRC member (Bmi1; a model is shown in Fig. 8c). A crucial role of the Twist1–Bmi1 pathway in HIF-1α-induced EMT and cell stemness properties is thereby elucidated. This information will be valuable for the prognostic prediction and treatment of hypoxic and metastatic cancers.

METHODS

Methods and any associated references are available in the online version of the paper at http://www.nature.com/naturecellbiology/

Note: Supplementary Information is available on the Nature Cell Biology website

ACKNOWLEDGEMENTS

We would like to thank M. C. Hung (M. D. Anderson Cancer Center) for critical comments on the manuscript. We thank L. E. Huang (University of Utah) for pHA-*HIF1α*(ΔODD) plasmid. We are grateful to T.Y. Chou and W.Y. Li of the Department of Pathology, Taipei Veterans General Hospital for providing advice on IHC analysis. This work was supported in part by National Science Council grants to M.H.Y. (96-2314-B-075-013 and 97-2314-B-010-003) and K.J.W.(97-2320-B-010-029), National Research Program for Genomic Medicine grants to K.J.W (DOH98-TD-G-111-027 and DOH99-TD-G-111-024); Taipei Veterans General Hospital grants to M.H.Y (VGH 98-C1-050; 98-ER2-008, 99-C1-077 and 99-ER2-007) and K.J.W (99-ER2-009), grants from Ministry of Education, Aim for the Top University Plan to M.H.Y (98A-C-T510 and 99A-C-T509) and to K.J.W (99A-C-T508), National Health Research Institutes grants to K.J.W (NHRI-EX-98-9611BI and NHRI-EX-99-9931BI) and a grant from Department of Health, Center of Excellence for Cancer Research at Taipei Veterans General Hospital (DOH99-TD-C-111-007) to M.H.Y.

AUTHOR CONTRIBUTION

M.H.Y., D.S.S.H. and K.J.W. conceived and designed the experiments. M.H.Y., D.S.S.H., H.J.W., H.Y.L. and W.H.Y. performed the experiments with the assistance of C.H.H for *in vivo* work. H.W.W. performed the bioinformatics analysis. M.H.Y., D.S.S.H. and K.J.W. analysed the data. M.H.Y. and K.J.W. wrote the paper with the assistance of O.S.K.L. and H.W.W. The treatment and sample collection of head-and-neck cancer patients were performed by S.Y.K., S.K.T., S.Y.C., C.H.T. and M.H.Y.

COMPETING FINANCIAL INTERESTS

The authors declare no competing financial interests.

Published online at http://www.nature.com/naturecellbiology
Reprints and permissions information is available online at http://npg.nature.com/reprintsandpermissions/

1. Thiery, J. P., Acloque, H., Huang, R. Y. & Nieto, M. A. Epithelial–mesenchymal transitions in development and disease. *Cell* **139,** 871–890 (2009).
2. Mani, S. A. *et al.* The epithelial–mesenchymal transition generates cells with properties of stem cells. *Cell* **133,** 704–715 (2008).
3. Morel, A. P. *et al.* Generation of breast cancer stem cells through epithelial–mesenchymal transition. *PLoS ONE* **3,** e2888 (2008).
4. Valk-Lingbeek, M. E., Bruggeman, S. W. & van Lohuizen, M. Stem cells and cancer: the polycomb connection. *Cell* **118,** 409–418 (2004).
5. Widschwendter, M. *et al.* Epigenetic stem cell signature in cancer. *Nat. Genet.* **39,** 157–158 (2007).
6. Molofsky, A. V. *et al.* Bmi-1 dependence distinguishes neural stem cell self-renewal from progenitor proliferation. *Nature* **425,** 962–967 (2003).
7. Iwama, A. *et al.* Enhanced self-renewal of haematopoietic stem cells mediated by the polycomb gene product Bmi-1. *Immunity* **21,** 843–851 (2004).
8. Sangiorgi, E. & Capecchi, M. R. Bmi1 is expressed *in vivo* in intestinal stem cells. *Nat. Genet.* **40,** 915–920 (2008).
9. Jacobs, J. J., Kieboom, K., Marino, S., Depinho, R. & van Lohuizen, M. The oncogene and polycomb-group gene *Bmi1* regulates cell proliferation and senescence through the *ink4a* locus. *Nature* **397,** 164–168 (1999).
10. Bruggeman, S. W. *et al.* Ink4a and Arf differentially affect cell proliferation and neural stem cell self-renewal in Bmi1-deficient mice. *Genes & Dev.* **19,** 1438–1443 (2005).
11. Czermin, B. *et al. Drosophila* Enhancer of Zeste/ESC complexes have a histone H3 methyltransferase activity that marks chromosomal polycomb sites. *Cell* **111,** 185–196 (2002).
12. Müller, J. *et al.* Histone methyltransferase activity of a *Drosophila* polycomb group repressor complex. *Cell* **111,** 197–208 (2002).
13. Min, J., Zhang, Y. & Xu, R. M. Structural basis for specific binding of polycomb chromodomain to histone H3 methylated at Lys 27. *Genes & Dev.* **17,** 1823–1828 (2003).
14. Bracken, A. P. *et al.* The polycomb group proteins bind throughout the *INK4A–ARF* locus and are disassociated in senescent cells. *Genes & Dev.* **21,** 525–530 (2007).
15. Jacobs, J. J. *et al.* Bmi-1 collaborates with c-Myc in tumorigenesis by inhibiting c-Myc-induced apoptosis via INK4a/ARF. *Genes Dev.* **13,** 2678–2690 (1999).
16. Leung, C. *et al.* Bmi1 is essential for cerebellar development and is overexpressed in human medulloblastomas. *Nature* **428,** 337–341 (2004).
17. Prince, M. E. *et al.* Identification of a subpopulation of cells with cancer stem cell properties in head and neck squamous cell carcinoma. *Proc. Natl Acad. Sci. USA.* **104,** 973–978 (2007).
18. Chiba, T. *et al.* The polycomb gene product BMI1 contributes to the maintenance of tumor-initiating side population cells in hepatocellular carcinoma. *Cancer Res.* **68,** 7742–7749 (2008).
19. Seiwert, T. Y. & Cohen, E. E. State-of-the-art management of locally advanced head and neck cancer. *Br. J. Cancer* **92,** 1341–1348 (2005).
20. Janssen, H. L., Haustermans, K. M., Balm, A. J. & Begg, A. C. Hypoxia in head and neck cancer: how much, how important? *Head Neck* **27,** 622–638 (2005).
21. Hoogsteen, I. J., Marres, H. A., Bussink, J., van der Kogel, A. J. & Kaanders, J. H. Tumor microenvironment in head and neck squamous cell carcinomas: predictive value and clinical relevance of hypoxic markers. A review. *Head Neck* **29,** 591–604 (2007).
22. Furlong, E. E., Andersen, E. C., Null, B., White, K. P. & Scott, M. P. Patterns of gene expression during *Drosophila* mesoderm development. *Science* **293,** 1629–1633 (2001).
23. Yang, J. *et al.* Twist, a master regulator of morphogenesis, plays an essential role in tumor metastasis. *Cell* **117,** 927–939 (2004).
24. Yang, M. H. *et al.* Direct regulation of TWIST by HIF-1α promotes metastasis. *Nat. Cell Biol.* **10,** 295–305 (2008).
25. Keith, B. & Simon, M. C. Hypoxia-inducible factors, stem cells and cancer. *Cell* **129,** 465–472 (2007).
26. Chen, Y. C. *et al.* Aldehyde dehydrogenase 1 is a putative marker for cancer stem cells in head and neck squamous cancer. *Biochem. Biophys. Res. Commun.* **385,** 307–313 (2009).
27. Huang, L. E., Gu, J., Schau, M. & Bunn, H. F. Regulation of hypoxia-inducible factor 1alpha is mediated by an O2-dependent degradation domain via the ubiquitin–proteasome pathway. *Proc. Natl Acad. Sci. USA.* **95,** 7987–7992 (1998).
28. Vermeulen, L. *et al.* Single-cell cloning of colon cancer stem cells reveals a multi-lineage differentiation capacity. *Proc. Natl Acad. Sci. USA.* **105,** 13427–13432 (2008).
29. Cao, Q. *et al.* Repression of E-cadherin by the polycomb group protein EZH2 in cancer. *Oncogene* **27,** 7274–7284 (2008).
30. Tamura, G. *et al.* E-Cadherin gene promoter hypermethylation in primary human gastric carcinomas. *J. Natl Cancer Inst.* **92,** 569–573 (2000).
31. Peinado, H., Ballestar, E., Esteller, M. & Cano, A. Snail mediates E-cadherin repression by the recruitment of the Sin3A/histone deacetylase 1 (HDAC1)/HDAC2 complex. *Mol. Cell Biol.* **24,** 306–319 (2004).
32. Hou, Z. *et al.* The LIM protein AJUBA recruits protein arginine methyltransferase 5 to mediate SNAIL-dependent transcriptional repression. *Mol. Cell Biol.* **28,** 3198–3207 (2008).
33. Herranz, N. *et al.* Polycomb complex 2 is required for E-cadherin repression by the Snail1 transcription factor. *Mol. Cell Biol.* **28,** 4772–4781 (2008).
34. Wellner, U. *et al.* The EMT-activator ZEB1 promotes tumorigenicity by repressing stemness-inhibiting microRNAs. *Nat. Cell Biol.* **11,** 1487–95 (2009).
35. Yang, M. H. & Wu, K. J. TWIST activated by hypoxia inducible factor-1 (HIF-1): implication in metastasis and development. *Cell Cycle* **7,** 2090–2096 (2008).
36. Li, J. *et al.* Oncoprotein Bmi-1 renders apoptotic resistance to glioma cells through activation of the IKK-nuclear factor-κB pathway. *Am. J. Pathol.* **176,** 699–709 (2010).
37. Vormittag, L. *et al.* Co-expression of Bmi-1 and podoplanin predicts overall survival in patients with squamous cell carcinoma of the head and neck treated with radio(chemo) therapy. *Int. J. Radiat. Oncol. Biol. Phys.* **73,** 913–918 (2009).
38. Gustafsson, M. V. *et al.* Hypoxia requires notch signaling to maintain the undifferentiated cell state. *Dev. Cell* **9,** 617–628 (2005).
39. Timmerman, L. A. *et al.* Notch promotes epithelial–mesenchymal transition during cardiac development and oncogenic transformation. *Genes Dev.* **18,** 99–115 (2004).
40. Androutsellis-Theotokis, A. *et al.* Notch signalling regulates stem cell numbers *in vitro* and *in vivo*. *Nature* **442,** 823–826 (2006).

DOI: 10.1038/ncb2099

METHODS

Cell lines, plasmids, stable transfection and oxygen deprivation. Human HNSCC cell lines, (FaDu, OECM-1, SAS and human embryonic kidney 293T; HEK-293T), were obtained from the American Type Culture Collection. The pcDNA3-*Bmi1* plasmid was generated by insertion of a 980-bp fragment of the full-length human *BMI1* cDNA into the *Bam*HI/*Not*I sites of the pcDNA3.1 vector. The plasmids for siRNA experiments were generated by inserting an oligonucleotide containing a specific siRNA target sequence or a scrambled sequence into the pSUPER vector (Supplementary Information, Table S6). The pFLAG-CMV, pFLAG-*TWIST1* and pcDNA3-*Slug* plasmids have been previously described[24,41]. Stable clones were generated by transfection of expression vectors and/or siRNA plasmids and selected by appropriate antibiotics. Oxygen deprivation used a hypoxic incubator with 1% O_2, 5% CO_2 and 94% N_2 for 18 h.

Protein extraction, western blot analysis, RNA extraction and quantitative real-time PCR. Protein extraction and western blot analysis were performed as previously described[42]. The antibodies used are listed in Supplementary Information, Table S7. RNA extraction was performed as previously described[42]. Quantitative real-time PCR was performed by the StepOnePlus real-time PCR system (Applied Biosystems) with the preset PCR programme, and GAPDH (glyceraldehyde 3-phosphate dehydrogenase) was applied as an internal control. The sequences of primers used for real-time PCR experiments are shown in Supplementary Information, Table S6.

Cloning of the regulatory regions of *BMI1* and *E-cadherin*, generation of the reporter construct, transient transfection and luciferase assays. The regulatory region of the *BMI1* and *E-cadherin* gene was cloned by PCR amplification of genomic DNA and inserted into the *Hind*III/*Bgl*II sites of the pXP2 vector to generate the *Bmi1–Luc*1000 and pXP2-*E-cadherin*(WT) parental constructs (Figs 2b and 7a and Supplementary Information, Tables S8 and S9). The *Bmi1–Luc*697 and *Bmi1–Luc*1000Mut constructs were made by deletion or mutation of the Twist1-binding site in *Bmi1–Luc*1000 (Fig. 2b). The pXP2-*E-cadherin*(mut-E1), pXP2-*E-cadherin*(mut-E1E2) and pXP2-*E-cadherin*(mut-E1E2E3) constructs were generated by mutation of one, two or three E-boxes of the *E-cadherin* promoter (Fig. 7a and Supplementary Information, Fig. S6a and Table S9).

The reporter constructs were co-transfected into HEK-293T, FaDu or OECM-1 cells with different expression or control vector(s), under normoxia or hypoxia, as indicated. A plasmid expressing the bacterial β-galactosidase gene (pCMV–*βGal*) was co-transfected in each experiment as an internal control for transfection efficiency. Cells were harvested after 48 h of transfection and luciferase activities were assayed as previously described[24]. The relative promoter activities were expressed as the fold-change in luciferase activity after normalization to β-galactosidase activity.

Electrophoretic mobility shift assay (EMSA). Oligonucleotides containing putative binding sequences of Twist1 were labelled with α^{32}P-dCTP and incubated with nuclear extracts harvested from HEK-293T cells, with or without *TWIST1* overexpression. Electrophoresis was performed and detected by a phosphoimager plate. For the supershift assay, the monoclonal antibody was added to the reaction mixture with a final dilution of 1:30 and incubated at 4 °C for 20 min. In the competition assay, excess amounts of unlabelled competitors were added before the labelled probes. The sequences of the probes used in EMSA are shown in Supplementary Information, Tables S8 and S9.

Standard and quantitative chromatin immunoprecipitation (ChIP and qChIP). Standard ChIP assays were performed as previously described[24]. For qChIP analysis, regions of interest were amplified from precipitated samples by real-time PCR. Each sample was assayed in triplicate, and the amount of precipitated DNA was calculated as the percentage of input sample[14]. The primers and antibodies used in ChIP and qChIP assays are listed in Supplementary Information, Tables S6 and S7, and the sequence information of ChIP and qChIP assays are shown in Supplementary Information, Tables S8–S10.

Flow-cytometric analysis of CD44 expression, ALDEFLUOR assay and side population analysis. To analyze CD44 expression, cells were resuspended and incubated with FITC-conjugated anti-CD44 antibody and evaluated with a FACSCalibur flow cytometer (BD Biosciences). ALDEFLUOR assay kit (#101700, Stem Cell Technologies) was used in the ALDEFLUOR assay[43]. A specific ALDH1 inhibitor, diethylaminobenzaldehyde, was used as a negative control, and cells were analysed with a FACSCalibur flow cytometer. The side population analysis was performed as previously described[18], and the cells were analysed by the FACSAria cell-sorter (BD Biosciences). FACSAria cell-sorting was also applied for sorting CD44- or ALDH1-positive cells.

Spheroids formation assay. Cells (1×10^4) were suspended in defined serum-free medium composed of DMEM/F-12 (Dulbecco's Modified Eagle Medium: Nutrient Mixture F-12; Gibco-BRL), N_2 supplement (R&D Systems), 10 ng ml^{-1} human recombinant bFGF (basic fibroblast growth factor; R&D Systems) and 10 ng ml^{-1} EGF (epidermal growth factor; R&D Systems). The spheroids were resuspended to form secondary and tertiary spheroids. The number of spheroids were counted after 14 days.

Soft-agar colony formation assay. Cells (5×10^3 or 1×10^4) of each clone were suspended in culture medium containing 0.3% agar (Sigma Chemical). The agar-cell mixture was plated on top of a bottom layer with 0.5% agar-medium mixture. After 14 days, viable colonies larger than 0.5 mm were counted.

Radiation treatment and cell-viability analysis. Cells were trypsinized and plated on dishes 16 h before irradiation. The gamma radiation was delivered by a Theratronic cobalt unit T-1000 (Theratronic International) at a dose rate of 1.1 Gy min^{-1}. Colonies were stained with crystal violet and counted 14 days after irradiation. A colony by definition had > 50 cells. The surviving fraction was calculated by dividing the number of colonies formed by the number of cells plated, multiplied by plating efficiency.

Array hybridization, data processing and bioinformatics analysis. The Affymetrix HG-U133 plus 2.0 whole genome array was used in this study. Total RNA collection, cRNA probe preparation, array hybridization, feature selection and computational analysis were performed as previously described[44,45]. The *q*-value was calculated to control the multiple testing errors in differential expression analysis, as previously described[45]. Classical multidimensional scaling (MDS) was generated to provide a visual impression of how the various sample groups are related[45]. The heat map was created by the dChip software. The array data were deposited on Gene Expression Omnibus, and the GEO numbers are: GSE19046 (data from FaDu cells transfected with pcDNA3, FaDu cells overexpressing *HIF1α*(ΔODD), FaDu cells overexpressing *TWIST1* or FaDu cells overexpressing *BMI1*; http://www.ncbi.nlm.nih.gov/geo/query/acc.cgi?token=vjwdxgqmsyycobg&acc=GSE19406), GSE 19471 (data from MSCs; http://www.ncbi.nlm.nih.gov/geo/query/acc.cgi?token=rdkxziycqcussls&acc=GSE19471). The array data of epithelial cells was obtained from the ArrayExpress database with the accession number: E-MEXP-993 (ref. 46).

Immunofluorescence-microscopy staining. The procedures were performed as previously described[47]. The characteristics of the antibodies used are listed in Supplementary Information, Table S7.

***In vivo* tumorigenicity assays.** All the animal protocols in this study were in accordance with the institutional animal welfare guideline of Taipei Veterans General Hospital. Different doses of cells were subcutaneously injected into 8-week-old BALB/C nude mice. Tumour incidence was monitored 6 weeks after injection.

Cell migration and invasion assay. A Boyden chamber (8-μm pore size) was used for *in vitro* migration and invasion assays. The procedures were performed as previously described[47].

Plasmid immunoprecipitation. The plasmid immunoprecipitation assay was performed as previously described[48]. Briefly, 5×10^6 HEK-293T cells were co-transfected with 0.5 μg of promoter plasmid (pXP2-E-cadherin(WT) or pXP2-E-cadherin(*mut*-E1E2E3)) and 5 μg of each expression vector (pFLAG-*TWIST1* and/or pcDNA3-*BMI1*). Empty vectors (pFLAG-CMV and/or pcDNA3.1) were used as a control for the transfection experiments. Cells were harvested and fixed at 30 h after transfection. The subsequent immunoprecipitation procedures were identical to ChIP assay described above. The binding activity of Twist1 or Bmi1 to the ectopic promoter was detected by quantitative PCR. Plasmid immunopre-

cipitation results were quantified relative to the input amount. The primers used in the plasmid immunoprecipitation experiment are shown in Supplementary Information, Table S6, and the antibodies used are listed in Supplementary Information, Table S7.

Co-immunoprecipitation assay. Nuclear extracts from FaDu cells overexpressing *TWIST1*-1 or *BMI1*-1 clones were incubated with anti-Twist1, anti-Bmi1 or control IgG overnight at 4 °C. We used the Thermo Scientific Crosslink IP Kit (Thermo Scientific) to prevent the interference of the co-imunoprecipitation results by the IgG bands. The immune complexes were incubated overnight with protein-A beads. The antibodies were absorbed onto immobilized protein-A and were chemically cross-linked. Then the target protein complexes were eluted and subjected to SDS–PAGE. After transfer, the membranes were blocked with blocking buffer, probed sequentially with a primary and a secondary antibody and developed. The antibodies used are listed in Supplementary Information, Table S7.

Study population, sample collection, immunohistochemistry (IHC) and cultivation of primary tumour cells. This study was approved by the Institutional Review Board of Taipei Veterans General Hospital. HNSCC patients (132) who had undergone surgical treatments at Taipei Veterans General Hospital between January 2003 and December 2006 were retrospectively analysed. The sample processing and IHC procedure were as previously described[42,47]. Interpretation of IHC was made independently by two specialists. For nuclear Twist1 and Bmi1, we graded the results into 0 to 3+ as previously described[24,49]: 0, no staining; 1+, 1–25%; 2+ 25–50%; and 3+, > 50% nuclear staining. Only 3+ was considered as a positive IHC result. Membranous E-cadherin and nuclear p16INK4a were interpreted as previously described[50,51]. All antibodies used for IHC are listed in Supplementary Information, Table S7. We collected samples from three HNSCC patients for primary cultivation of tumour cells. The tumour were dissociated in trypsin and collagenase then cultured in RPMI medium containing 10% fetal bovine serum. Cytokeratin expression was used to confirm the epithelial origin of HNSCC cells.

Equipments and settings. Raw TIFF images were merged in Adobe Photoshop (Adobe Systems) without background subtraction. For histology and immunohistochemistry, the images were captured by an Olympus BX51 High Class System microscope (Olympus) equipped with an Olympus DP71 microscope digital camera, Olympus U Plan FL ×10 and ×40 objectives, and Olympus WHB ×10 eyepieces. The acquisition software was Olympus DP controller (Olympus). The depth of captured image was 10 bit. For immunofluorescence microscopy, the images were captured by a Nikon ECLIPSE 50i microscope (Nikon) equipped with Media Cybernetics Evolution VF digital camera, Nikon Plan Fluor ×40 objective, and Nikon CFI ×10 eyepieces. The acquisition software was Image-Pro Plus, version 5.1(Media Cybernetics). The depth of captured image was 12 bit.

Statistical analysis. The independent Student's *t*-test was used to compare the continuous variables between two groups, and the chi-squared test was applied for comparison of dichotomous variables. The Kaplan-Meier estimation method was used for overall survival analysis, and a log-rank test was used to compare differences. The level of statistical significance was set at 0.05 for all tests.

41. Huang, C. H. *et al.* Regulation of membrane-type 4 matrix metalloproteinase (MT4-MMP) by SLUG contributes to hypoxia-mediated metastasis. *Neoplasia* **11,** 1371–1382 (2009).
42. Yang, M. H. *et al.* Increased *NBS1* expression is a marker of aggressive head and neck cancer and overexpression of *NBS1* contributes to transformation. *Clin. Cancer Res.* **12,** 507–515 (2006).
43. Ginestier, C. *et al.* ALDH1 is a marker of normal and malignant human mammary stem cells and a predictor of poor clinical outcome. *Cell Stem Cell* **1,** 555–567 (2007).
44. Huang, T. S. *et al.* Functional network reconstruction reveals somatic stemness genetic maps and dedifferentiation-like transcriptome reprogramming induced by GATA2. *Stem Cells* **26,** 1186–1201 (2008).
45. Wang, H. W. *et al.* Kaposi sarcoma herpesvirus-induced cellular reprogramming contributes to the lymphatic endothelial gene expression in Kaposi sarcoma. *Nat. Genet.* **36,** 687–693 (2004).
46. Birnie R. *et al.* Gene expression profiling of human prostate cancer stem cells reveals a pro-inflammatory phenotype and the importance of extracellular matrix interactions. *Genome Biol.* **9,** R83 (2008).
47. Yang, M. H. *et al.* Overexpression of NBS1 induces epithelial–mesenchymal transition and co-expression of NBS1 and Snail predicts metastasis of head and neck cancer. *Oncogene* **26,** 1459–1467 (2007).
48. Ainbinder, E., Amir-Zilberstein, L., Yamaguchi, Y., Handa, H. & Dikstein, R. Elongation inhibition by DRB sensitivity-inducing factor is regulated by the A20 promoter via a novel negative element and NF-κB. *Mol. Cell Biol.* **24,** 2444–2454 (2004).
49. Kang, M. K. *et al.* Elevated *Bmi-1* expression is associated with dysplastic cell transformation during oral carcinogenesis and is required for cancer cell replication and survival. *Br. J. Cancer* **96,** 126–133 (2007).
50. Foschini, M. P. *et al.* E-cadherin loss and Delta Np73L expression in oral squamous cell carcinomas showing aggressive behavior. *Head Neck* **30,** 1475–1482 (2008).
51. Kumar, B. *et al.* EGFR, p16, HPV Titer, Bcl-xL and p53, sex, and smoking as indicators of response to therapy and survival in oropharyngeal cancer. *J. Clin. Oncol.* **26,** 3128–3137 (2008).

nature cell biology

DOI: 10.1038/ncb2099

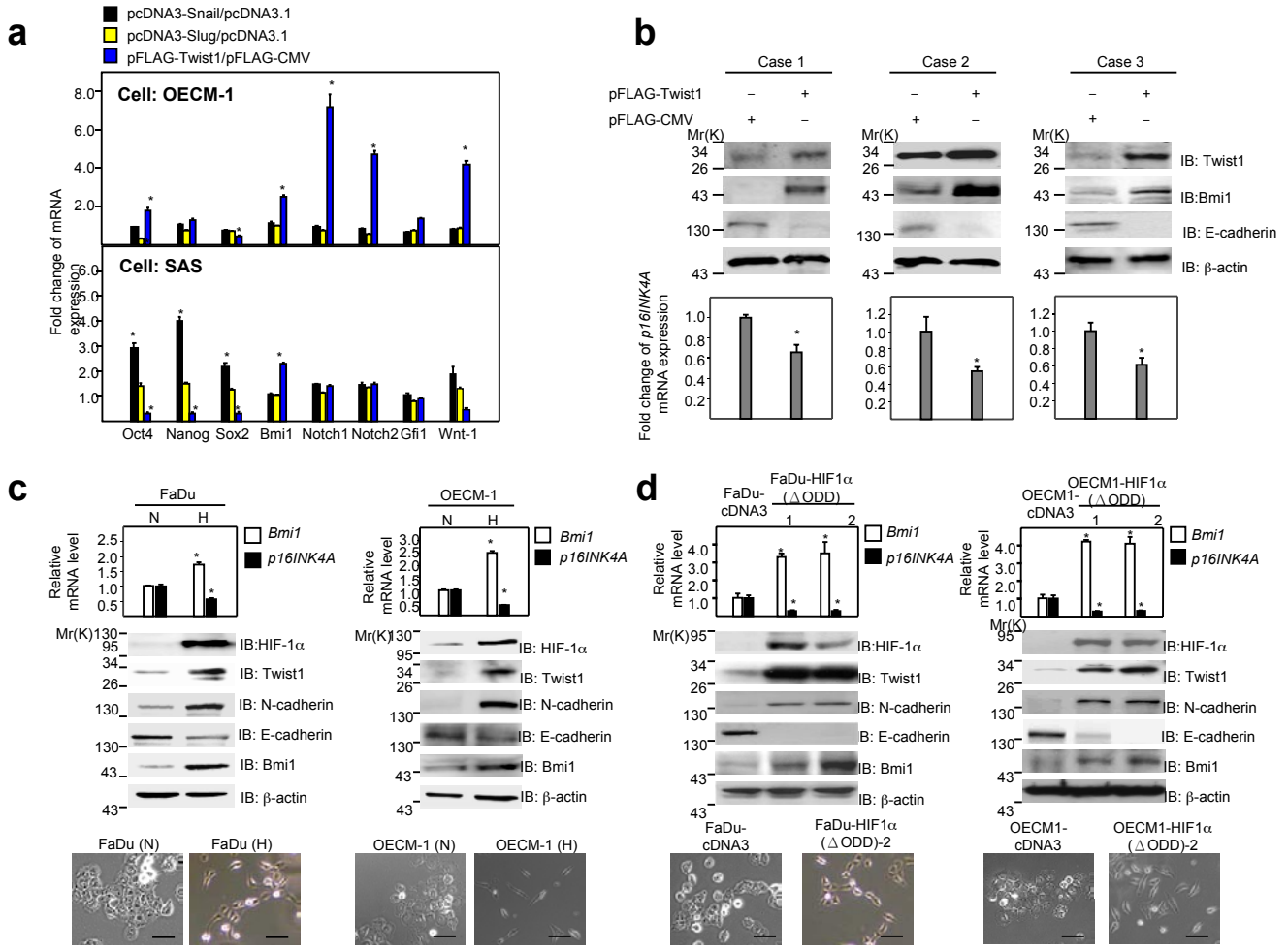

Figure S1 Overexpression of Twist1 upregulates Bmi1 in HNSCC cells, and hypoxia or overexpression of HIF-1α induces EMT and upregulates Bmi1. (a) Fold-change of mRNA levels of different stemness-related genes in OECM-1 cells (upper panel) or SAS cells (lower panel) transfected with pcDNA3-Snail, pcDNA3-Slug or pFLAG-Twist1. Transfection of an empty vector (pcDNA3.1 or pFLAG-CMV) was applied as a control in each experiment. Data represents means ± S.E.M. (n=3). An asterisk (*) indicates $P < 0.001$ (Student's *t*-test). (b) Upper: Western blot analysis of Twist1, Bmi1 and E-cadherin expression in primary HNSCC cells transfected with pFLAG-Twist1 vs. control vector. β-actin was used as a loading control. Lower: fold-change of mRNA levels of *p16INK4A* in of primary HNSCC cells transfected with pFLAG-Twist1 vs. control vector. Data represents means ± S.E.M. (n=3). An asterisk (*) indicates $P < 0.01$ between cells transfected with pFLAG-Twist1 and pFLAG-CMV (Student's *t*-test). (c) Fold change of mRNA levels of *Bmi1* and *p16INK4A* (upper), Western blot analysis of HIF-1α, Twist1 N-cadherin, E-cadherin and Bmi1 (middle), and phase-contrast images (lower) of FaDu and OECM-1 cells under normoxia (N) vs. hypoxia (H). Scale bars = 50 μm. Data represents means ± S.E.M. (n=3). An asterisk (*) indicates $P <$ 0.001 between normoxia and hypoxia (Student's *t*-test). (d) Fold change of mRNA levels of *Bmi1* and *p16INK4A* (upper), Western blot analysis of HIF-1α, Twist1 N-cadherin, E-cadherin and Bmi1 (middle), and phase-contrast images (lower) of FaDu and OECM-1 cells overexpressing HIF-1α (FaDu-HIF1α(ΔODD) and OECM1-HIF1α(ΔODD)) vs. control (FaDu-cDNA3 and OECM1-cDNA3). Scale bars = 50 μm. Data represents means ± S.E.M. (n=3). An asterisk (*) indicates $P < 0.001$ between cells expressing HIF-1α and control vector (Student's *t*-test).

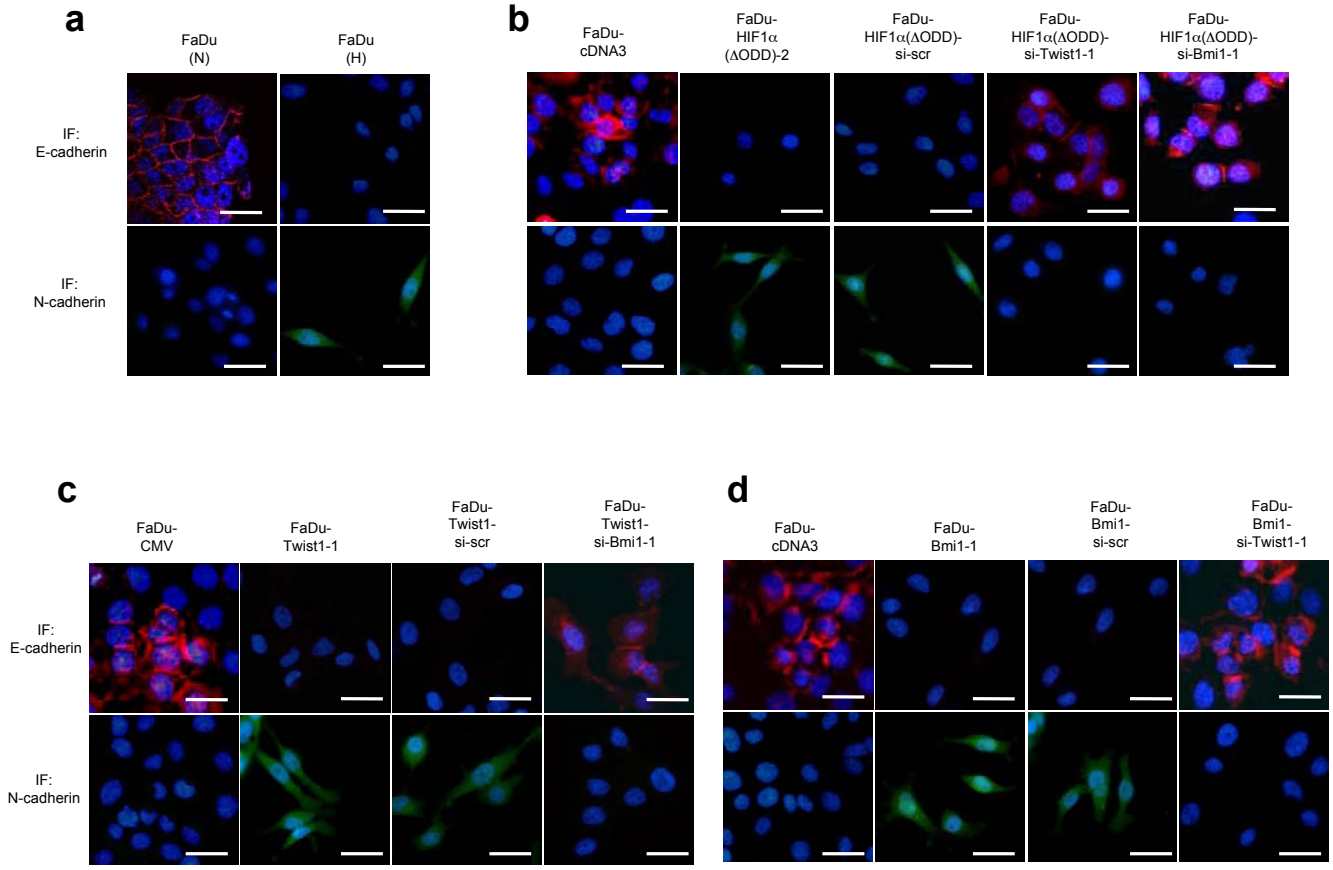

Figure S2 Induction of a mesenchymal phenotype by hypoxia or overexpression of HIF-1α or Twist1 or Bmi1, and suppression of Twist1 or Bmi1 reverses EMT in FaDu cells. (a) Immunofluorescent staining of E-cadherin (red) and N-cadherin (green) in FaDu cells under normoxia (N) or hypoxia (H). (b) Immunofluorescent staining of E-cadherin (red) and N-cadherin (green) in FaDu-cDNA3, FaDu-HIF1α(ΔODD), FaDu-HIF1α(ΔODD) receiving siRNA against Twist1 (FaDu-HIF1α(ΔODD)-si-Twist1), Bmi1 (FaDu-HIF1α(ΔODD)-si-Bmi1) or a scrambled control (FaDu-HIF1α(ΔODD)-si-scr). (c) Immunofluorescent staining of E-cadherin (red) and N-cadherin (green) in FaDu-CMV, FaDu-Twist1, FaDu-Twist1 receiving siRNA against Bmi1 (FaDu-Twist1-si-Bmi1) or a scrambled control (FaDu-Twist1-si-scr). (b) Immunofluorescent staining of E-cadherin (red) and N-cadherin (green) in FaDu-cDNA3, FaDu-Bmi1, FaDu-Bmi1-si-scr and FaDu-Bmi1-si-Twist1. The blue signal represented nuclear DNA staining by Hoechst 33342. Scale bars = 50 μm in each panel.

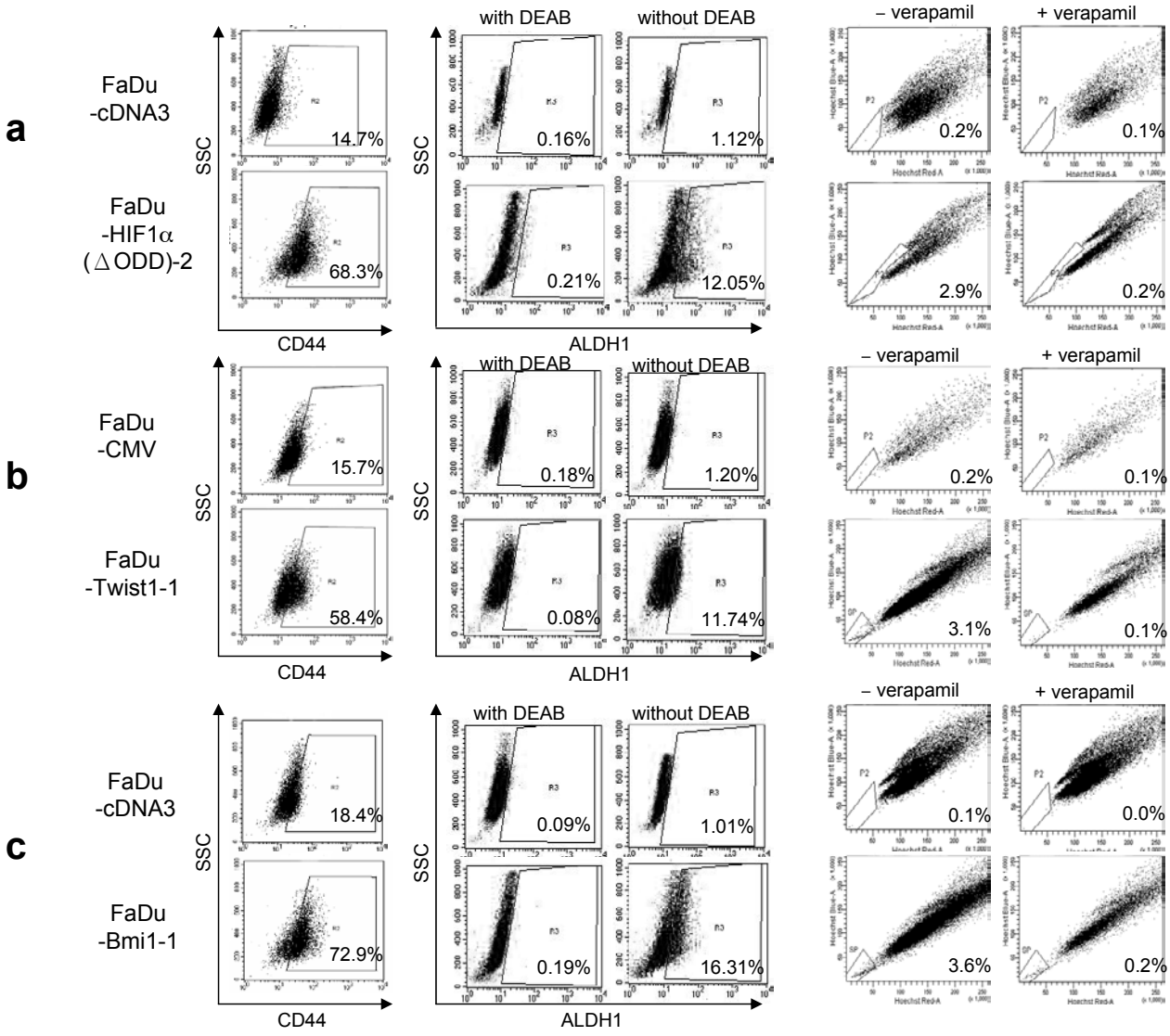

Figure S3 Representative results of flow-cytometric analysis. (a)-(c) Representative data of Fig. 3c. Analysis CD44 expression (left), ALDH1 activity and side population cells in FaDu-HIF1α(ΔODD)-2 vs. FaDu-cDNA3 (a), FaDu-Twist1-1 vs. FaDu-CMV (b), and FaDu-Bmi1-1 vs. FaDu-cDNA3 (c). (d)-(h) Representative data of Fig. 4c. Analysis of CD44 (left), ALDH1 activity (middle), and side population cells (right) of FaDu-CMV (d), FaDu-Twist1-1 (e), FaDu-Twist-si-scr (f), FaDu-Twist-si-Bmi1-1 (g) and FaDu-Twist-si-Bmi1-2 (h). (i)-(m) Representative data of Fig. 4g. Analysis of CD44 (left), ALDH1 activity (middle), and side population cells (right) of FaDu-cDNA3 (i), FaDu-Bmi1-1 (j), FaDu-Bmi1-si-scr (k), FaDu-Bmi1-si-Twist1-1 (l) and FaDu-Bmi1-si-Twist1-2 (m). For ALDEFLUOR assay, cells incubated with ALDEFLUOR substrate and diethylaminobenzaldehyde (DEAB), a specific inhibitor of ALDH1, were used to define the ALDEFLUOR-positive region. For analysis of side population (SP) cells, cells were treated with verapamil and the SP cells disappeared after treatment of verapamil. The percentages of CD44-positive, ALDH1-positive, and SP cells were shown in the right lower quadrant of each panel.

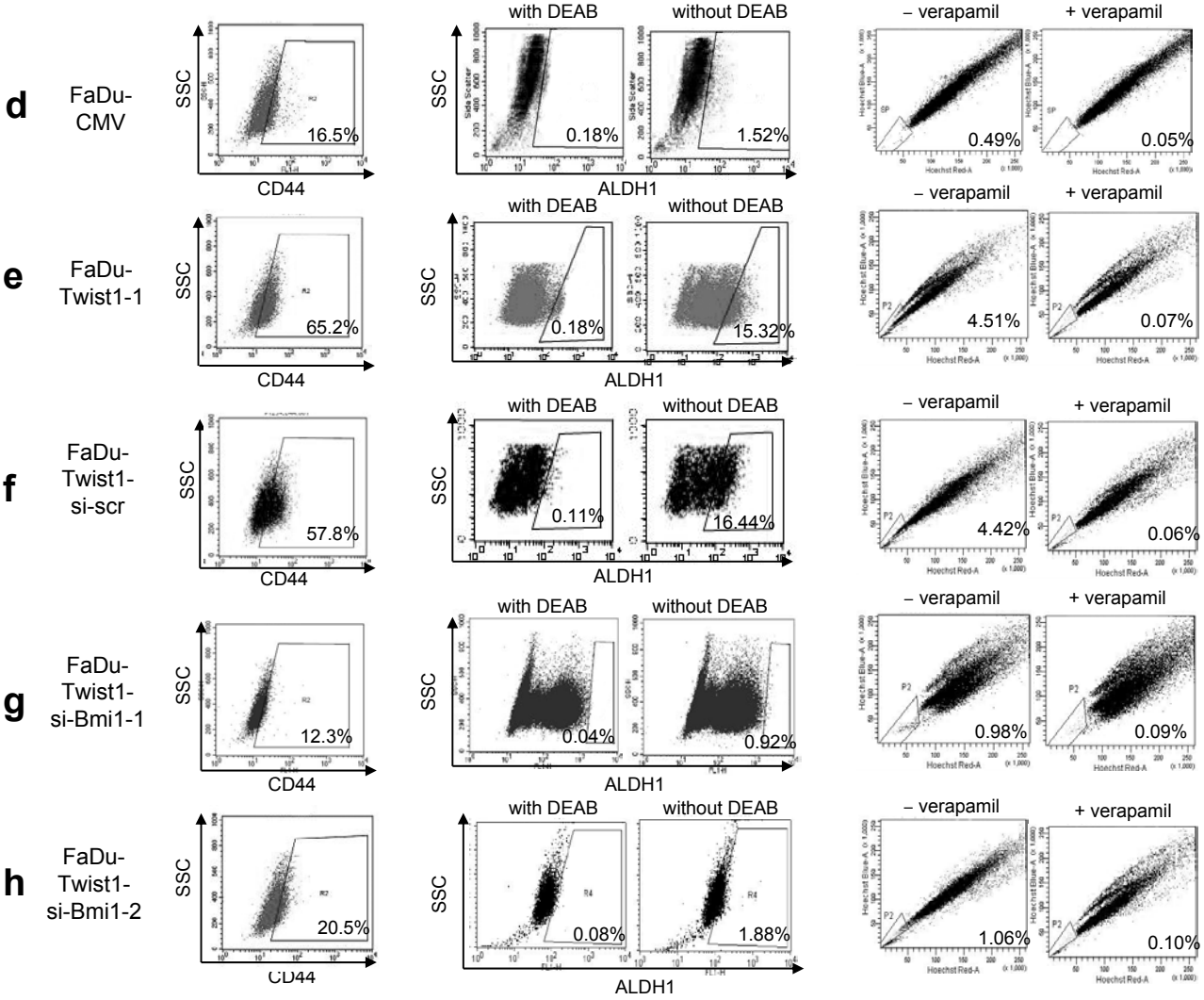

Figure S3 continued

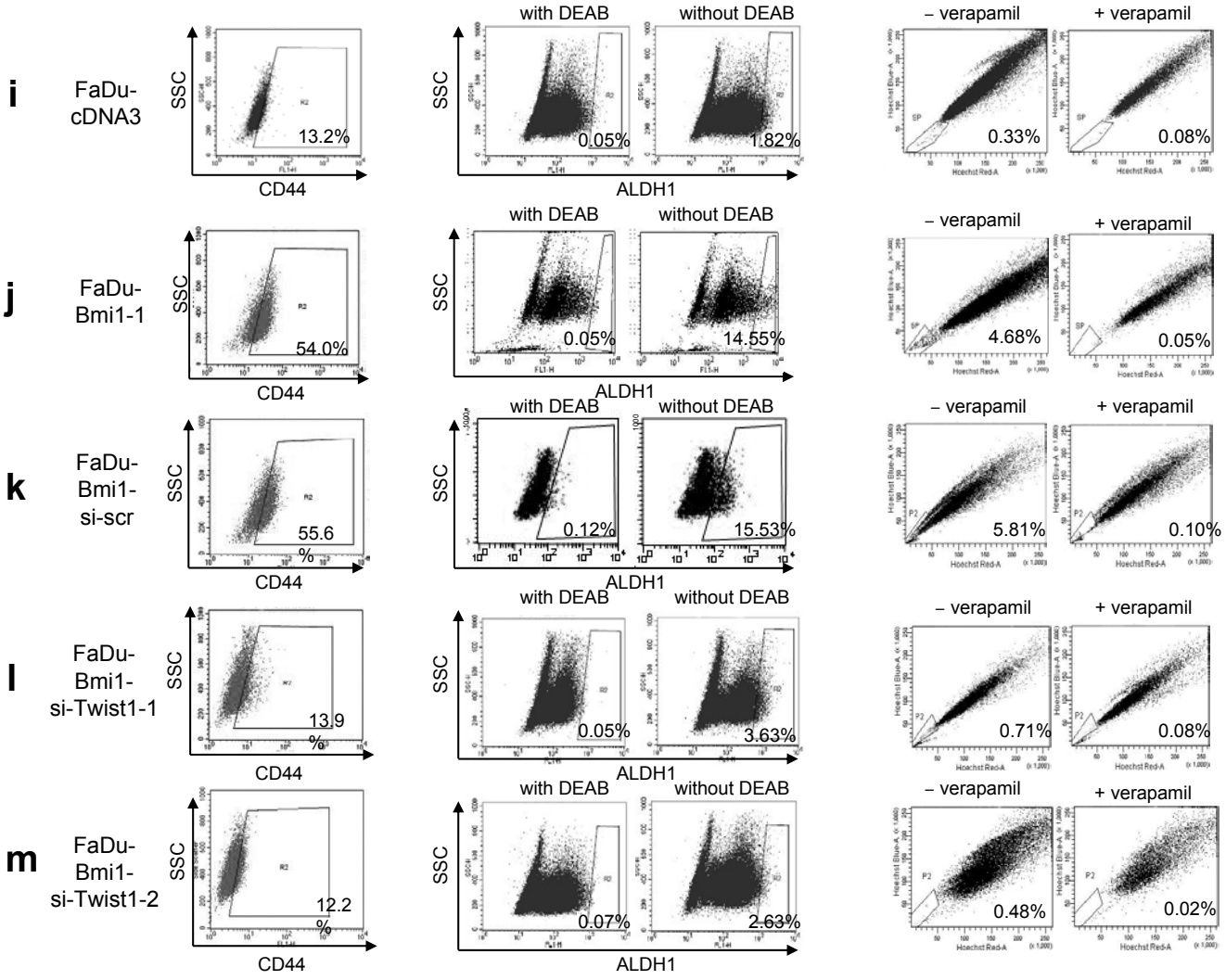

Figure S3 continued

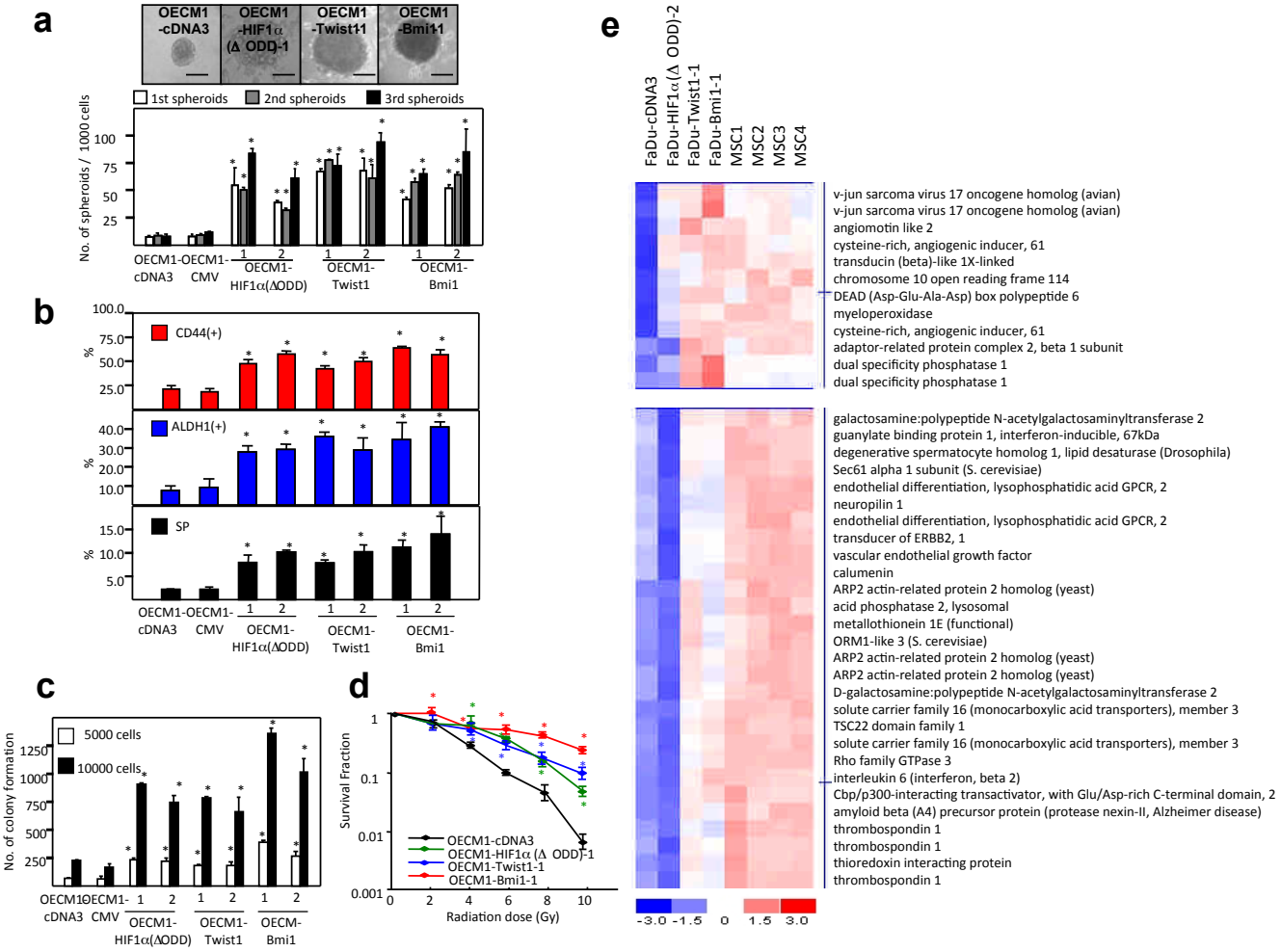

Figure S4 Overexpression of HIF-1α or Twist1 or Bmi1 in OECM-1 cells promotes stem-like properties, and a heatmap shows the differential gene expression in FaDu cells expressing HIF-1α or Twist1 or Bmi1. (a) Upper: representative pictures of spheroids of spheroid formation assay in OECM-1 cells overexpressing HIF-1α, Twist1 or Bmi1 and control clones. Scale bars = 100 μm. Lower: quantification of spheroid formation assay. Data represents means ± S.E.M. (n=3). An asterisk (*) indicates $P < 0.001$ compared with OECM1-cDNA3 (Student's *t*-test). (b) Percentage of CD44-positive (upper), ALDH1-positive (middle), and side population (SP) cells (lower) in OECM-1 overexpressing HIF-1α, Twist1 or Bmi1 and control clones. Data represents means ± S.E.M. (n=3). An asterisk (*) indicates $P < 0.001$ compared with OECM1-cDNA3 (Student's *t*-test). (c) Soft agar colony formation assay of OECM-1 cells overexpressing HIF-1α, Twist1 or Bmi1 and control clones. Data represents means ± S.E.M. (n=3). An asterisk (*) indicates $P < 0.001$ compared with OECM1-cDNA3 (Student's *t*-test). (d) Survival fraction of OECM-1 cells overexpressing HIF-1α, Twist1 or Bmi1 and control clones after irradiation treatment. Data represents means ± S.E.M. (n=3). An asterisk (*) indicates $P < 0.001$ compared with OECM1-cDNA3 (Student's *t*-test). (e) A heatmap shows the changes in gene expression of FaDu-HIF1α(ΔODD), FaDu-Twist1 and FaDu-Bmi1 ($q < 0.01$). The upper panel listed the genes commonly expressed between mesenchymal stem cells (MSCs), FaDu-HIF1α(ΔODD), FaDu-Twist1 and FaDu-Bmi1; whereas the lower panel showed the common genes between MSCs, FaDu-Twist1 and FaDu-Bmi1. Genes in red, up-regulated; in blue, down. MSC1, MSC2, MSC3 and MSC4 indicate results from four independent mesenchymal stem cell cultivations.

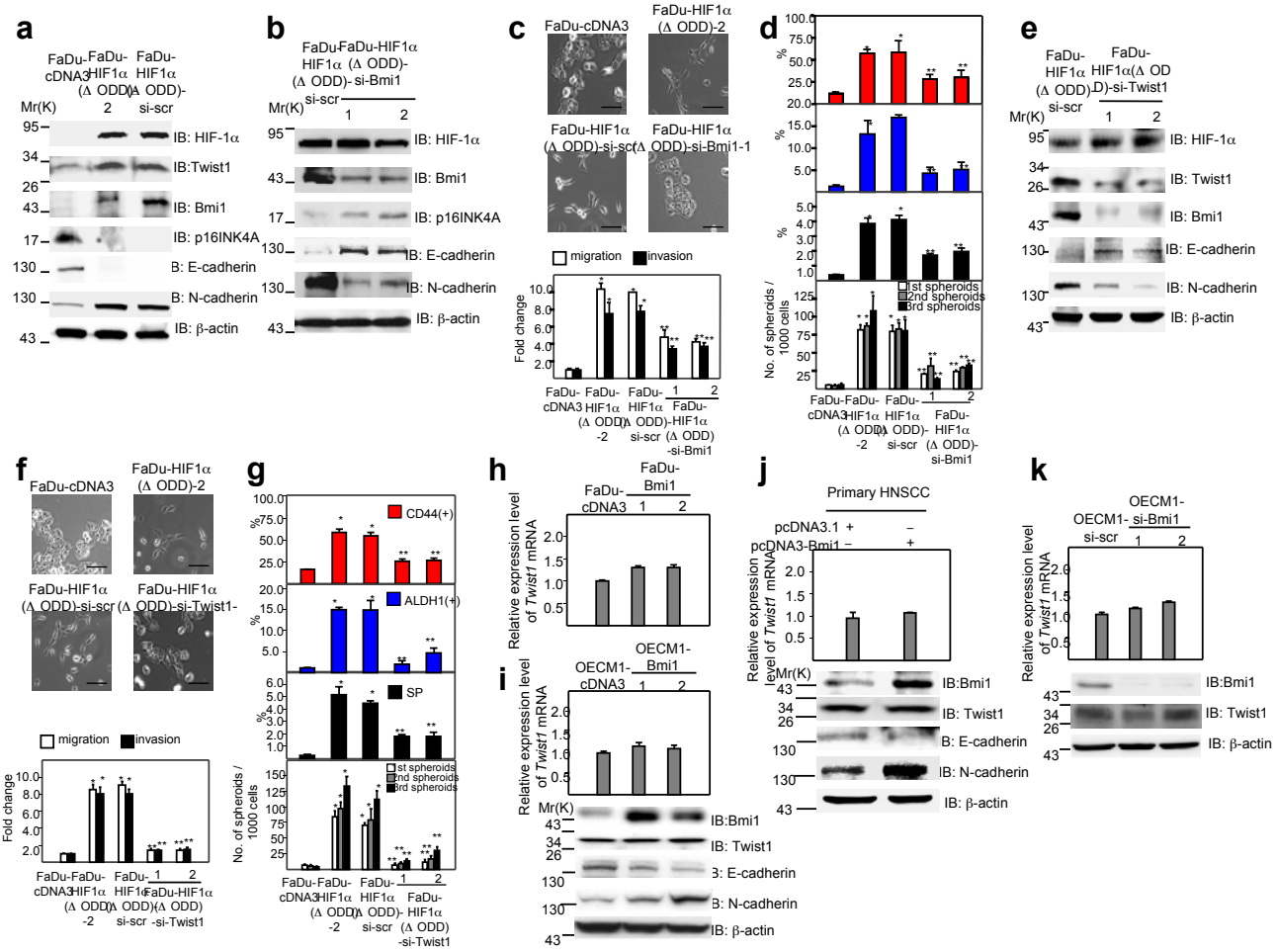

Figure S5 Repression of *Bmi1* or *Twist1* reverses EMT and stem-like properties of FaDu-HIF1α(ΔODD), and Bmi1 does not influence Twist1 expression in HNSCC. (a) Western blot analysis of HIF-1α, Twist1, Bmi1, p16INK4A, E-cadherin and N-cadherin expression in FaDu-cDNA3 vs. FaDu-HIF1α(ΔODD) vs. FaDu-HIF1α(ΔODD)-si-scr. (b) Western blot results of HIF-1α, Bmi1, p16INK4A, E-cadherin and N-cadherin in FaDu-HIF1α(ΔODD)-si-scr and FaDu-HIF1α(ΔODD)-si-Bmi1. (c) Upper: phase-contrast images of FaDu-cDNA3, FaDu-HIF1α(ΔODD), FaDu-HIF1α(ΔODD)-si-scr and FaDu-HIF1α(ΔODD)-si-Bmi1. Scale bars = 50 μm. Lower: quantification of migration and invasion assay. Data represents means ± S.E.M. (n=3). (d) Percentages of CD44-positive, ALDH1-positive, side population cells and the spheroid-forming capacity of FaDu-cDNA3, FaDu-HIF1α(ΔODD), FaDu-HIF1α(ΔODD)-si-scr and FaDu-HIF1α(ΔODD)-si-Bmi1. Data represents means ± S.E.M. (n=3). In (c) and (d), $*P < 0.001$ for FaDu-HIF1α(ΔODD) or FaDu-HIF1α(ΔODD)-si-scr vs. FaDu-cDNA3. $**P < 0.001$ for FaDu-HIF1α(ΔODD)-si-Bmi1 vs. FaDu- HIF1α(ΔODD)-si-scr (Student's *t*-test). (e) Western blot analysis of HIF-1α, Twist1, Bmi1, E-cadherin and N-cadherin expression in FaDu-HIF1α(ΔODD)-si-scr vs. FaDu-HIF1α(ΔODD)-si-Twist1. (f) Upper: phase-contrast images of FaDu-cDNA3, FaDu-HIF1α(ΔODD), FaDu-HIF1α(ΔODD)-si-scr and FaDu-HIF1α(ΔODD)-si-Twist1. Scale bars = 50 μm. Lower: quantification of migration and invasion assay. Data represents means ± S.E.M. (n=3). (g) Percentages of CD44-positive, ALDH1-positive, side population cells and the spheroid-forming capacity of FaDu-cDNA3, FaDu-HIF1α(ΔODD), FaDu-HIF1α(ΔODD)-si-scr and FaDu-HIF1α(ΔODD)-si-Twist1. Data represents means ± S.E.M. (n=3). In (f) and (g), $*P < 0.001$ for FaDu-HIF1α(ΔODD) or FaDu-HIF1α(ΔODD)-si-scr vs. FaDu-cDNA3. $**P < 0.001$ for FaDu-HIF1α(ΔODD)-si-Twist1 vs. FaDu- HIF1α(ΔODD)-si-scr (Student's *t*-test). (h) Relative *Twist1* mRNA level in FaDu-cDNA3 vs. FaDu-Bmi1. Data represents means ± S.E.M. (n=3). (i) Upper: relative *Twist1* mRNA level in OECM1-cDNA3 vs. OECM1-Bmi1. Data represents means ± S.E.M. (n=3). Lower: Western blot analysis of Twist1, Bmi1, E-cadherin and N-cadherin in OECM1-cDNA3 vs. OECM1-Bmi1. (j) Upper: relative *Twist1* mRNA level in primary HNSCC cells transfected with pcDNA3-Bmi1 vs. pcDNA3.1. Data represents means ± S.E.M. (n=3). Lower: Western blot analysis of Twist1, Bmi1, E-cadherin and N-cadherin in primary HNSCC cells transfected with pcDNA3-Bmi1 vs. pcDNA3.1. (k) Upper: relative *Twist1* mRNA level of OECM1-si-Bmi1 vs. OECM1-si-scr. Data represents means ± S.E.M. (n=3). Lower: Western blot analysis of Twist1 and Bmi1 in OECM1-si-scr vs. OECM1-si-Bmi1. β-actin was used as a loading control in Western blot analysis. scr, scrambled sequence.

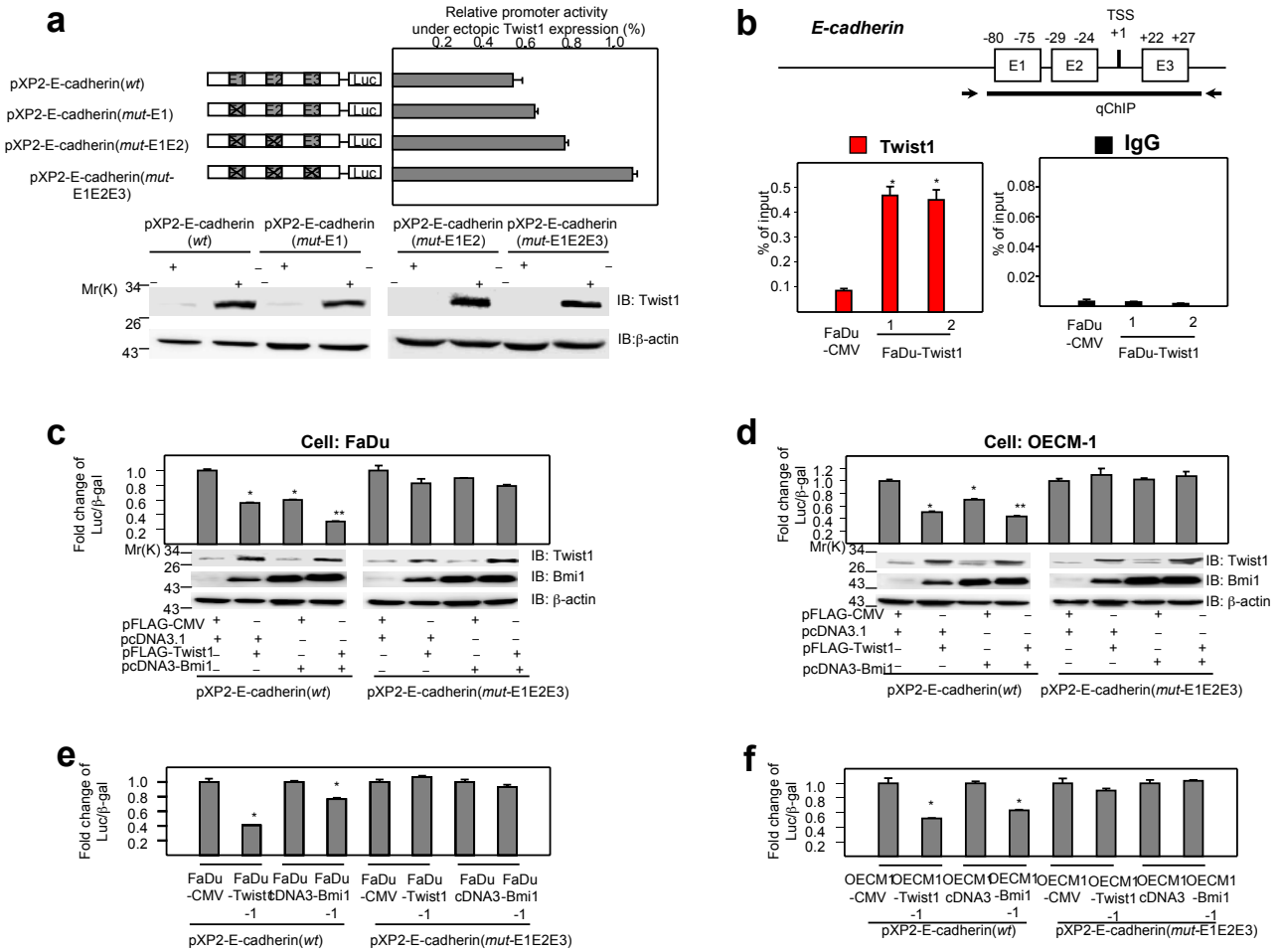

Figure S6 Direct repression of *E-cadherin* transcription by Twist1-containing complex, and repression of *E-cadherin* promoter activity by Twist1 and Bmi1 in HNSCC cells. (a) Upper: representation of the reporter constructs used in transient transfection assays (left), and promoter activity assay in HEK-293T cells co-transfected with the different promoter construct and a Twist1 expression vector or an empty vector. The promoter activity was estimated as luciferase activity/β-galactosidase. Data are presented as the relative promoter activity under ectopic Twist1 expression as the percentage of the activity of the same reporter transfected with an empty vector. Data represents means ± S.E.M. (n=3). Lower: Western blot results to indicate the expression of Twist1 under different transfection. (c) Upper: schematic representation of the PCR-amplified region of *E-cadherin* promoter in qChIP assay. Lower: qChIP results of FaDu-CMV vs. FaDu-Twist1. The irrelevant IgG was applied as a control of qChIP experiment. The binding activity of each protein wad presented as percentages of total input. Data represents means ± S.E.M. (n=3). $*P < 0.001$ between FaDu-Twist1 and FaDu-CMV (Student's *t*-test). (c),(d) Promoter activity assay of FaDu (c) and OECM-1 (d) co-transfected with the promoter and the expression vector(s) or the empty vector(s). Luciferase activity/β-galactosidase in cells transfected with empty vectors pFLAG-CMV/pcDNA3.1 was applied as the baseline control for the experiments using the same promoter. Western blot results were shown to indicate the expression levels of Twist1 and Bmi1 under various conditions. Data represents means ± S.E.M. (n=3).$*P < 0.001$ between cells transfected with single expression vector (pFLAG-Twist1 or pcDNA3-Bmi1) and the empty vector. $**P < 0.001$ between cells transfected with pFLAG-Twist1 and pFLAG-Twist1+pcDNA3-Bmi1 (Student's *t*-test). (e),(f) Promoter activity assay of stable cell lines. FaDu (e) and OECM-1 (f) cells which stably express Twist1 versus control vector (FaDu-CMV vs. FaDu-Twist1-1; OECM1-CMV vs. OECM1-Twist1-1), or stably express Bmi1 versus control vector (FaDu-cDNA3 vs. FaDu-Bmi1-1; OECM1-cDNA3 vs. OECM1-Bmi1-1) were transfected with different promoter construct, and the promoter activity was estimated as luciferase activity/β-galactosidase. Data represents means ± S.E.M. (n=3).$*P < 0.001$ between cells stably expressed Twist1 or Bmi1 vs. an empty vector control (Student's *t*-test).

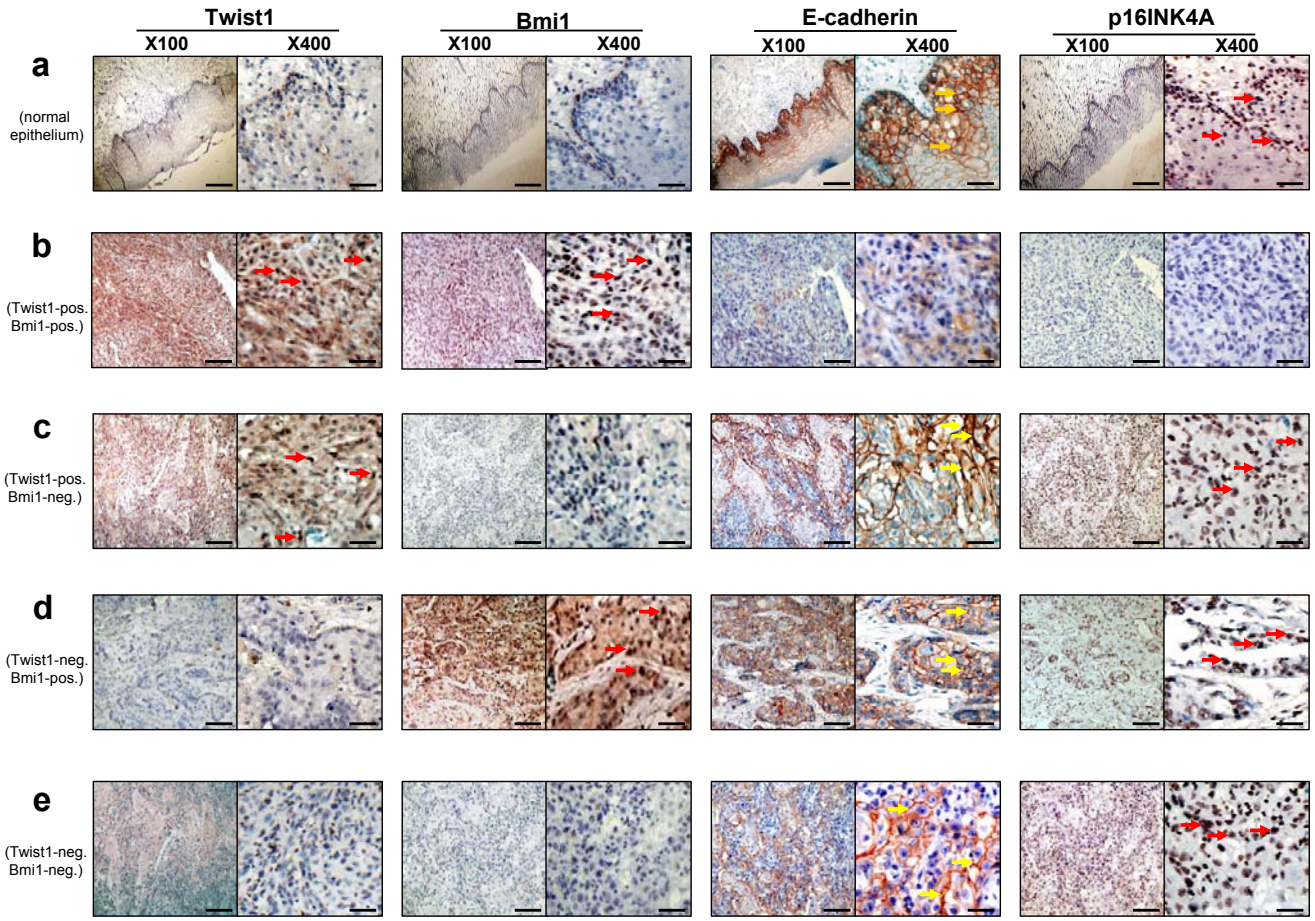

Figure S7 Representative pictures of the immunohistochemistry analyses of Twist1, Bmi1, E-cadherin and p16INK4A in normal oral epithelium (a), a Twist1-positve/Bmi1-positive case (b), a Twist1-positive/Bmi1-negative case (c), a Twist1-negative/Bmi1-positive case (d), and a Twist1-negative/Bmi1-negative case (e). The membranous E-cadherin expression is indicated by yellow arrows, whereas the nuclear expression of Twist1, Bmi1 and p16INK4A is indicated by red arrows. Scale bars = 500 μm (x100) and 100 μm (x400). pos., positive; neg., negative.

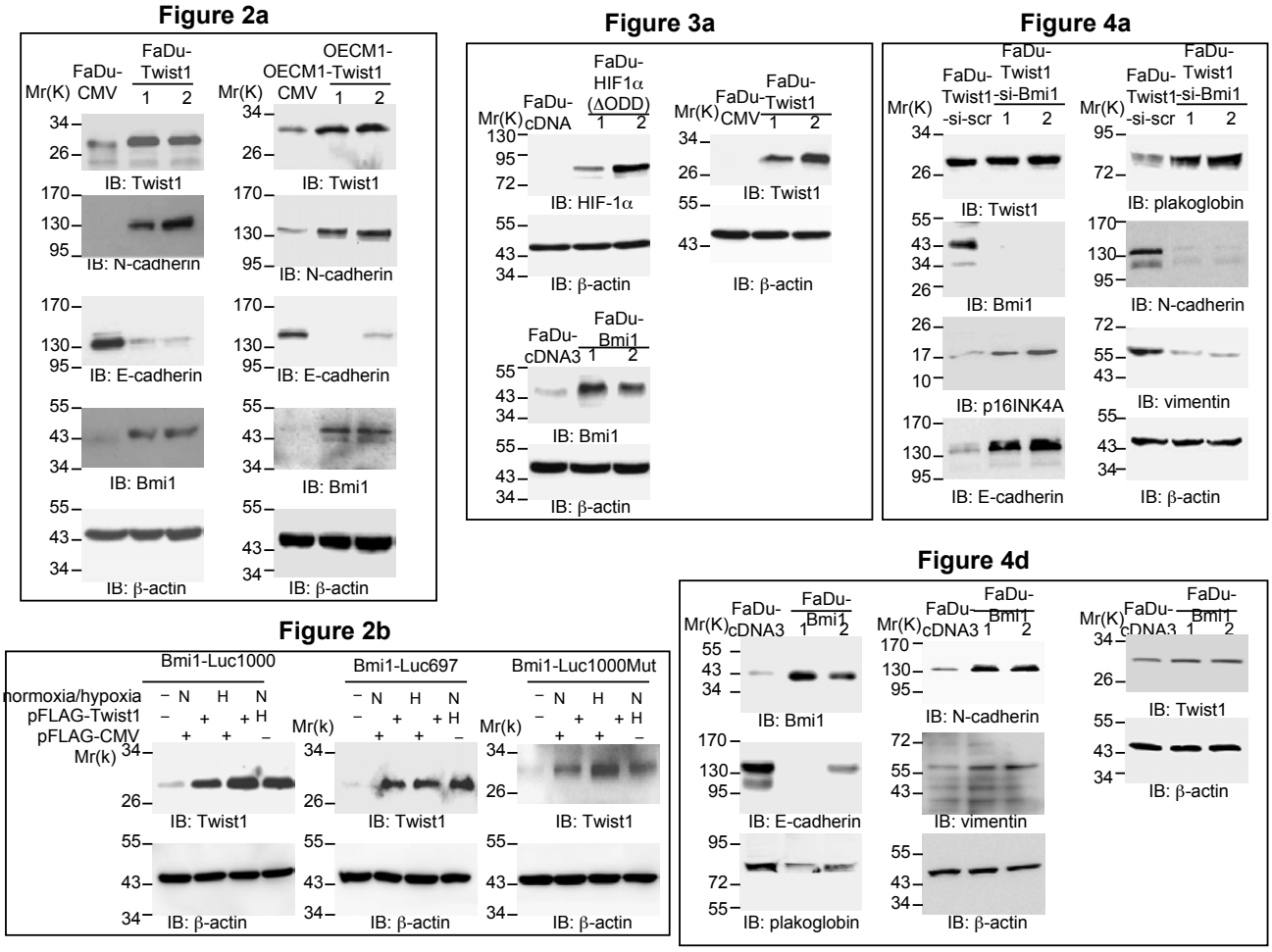

Figure S8 Full length blots of the Western data shown in the regular Figures 2a, 2b, 3a, 4a, 4d, 4e, 7a and 7d.

Figure 4e

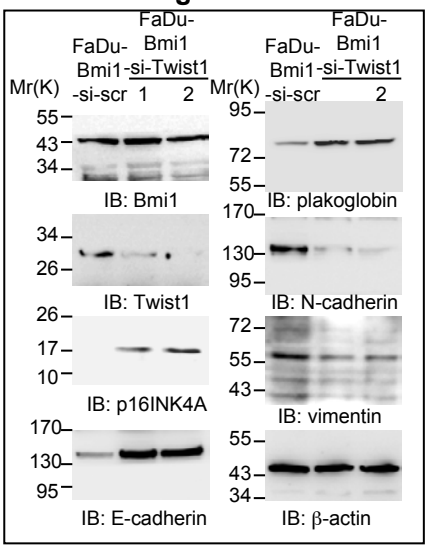

Figure 7a

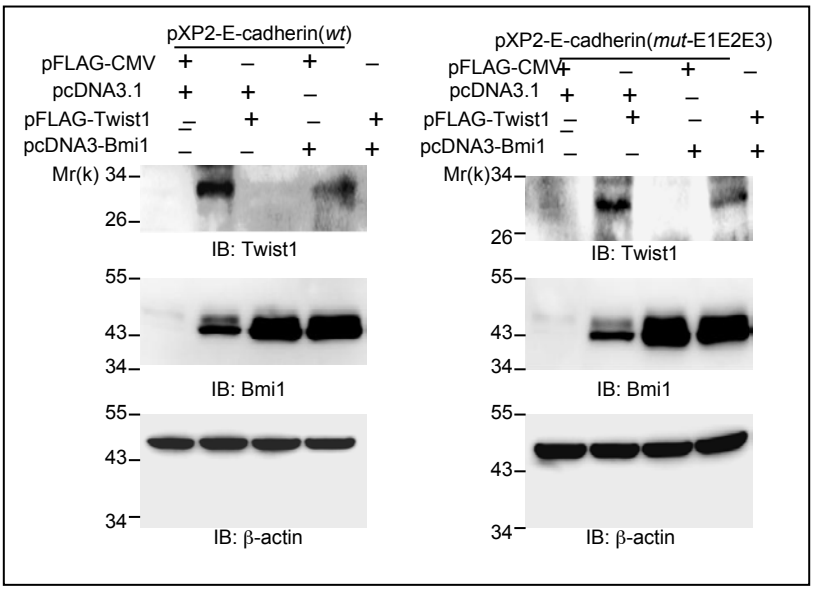

Figure 7d

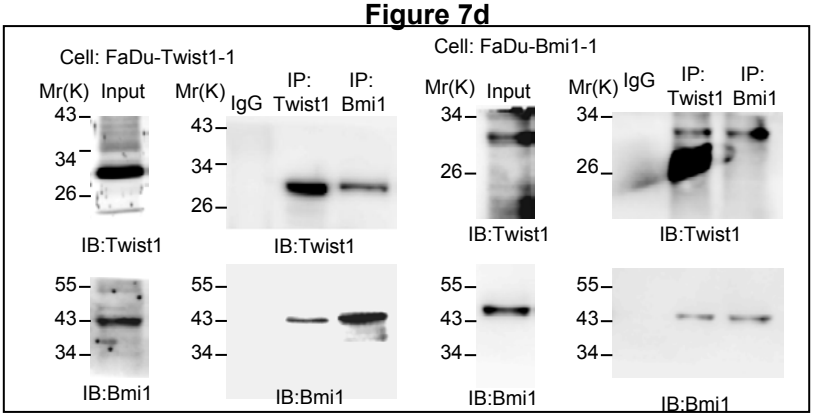

Figure S8 continued